Spectroscopy®

Solutions for Materials Analysis

Spectroscopy®

Solutions for Materials Analysis

www.spectroscopyonline.com

CELEBRATING OUR
Spectroscopy
★ 30TH YEAR ★

Elemental Analysis of Goji Berries

Why Spectral Interpretation Needs To Be Taught

LIBS Measurement of Geological Samples

UBM

SENSING CHANGE
APPLICATIONS FOR A BETTER WORLD

Spectroscopy ®

UBM

CONTENTS

Spectroscopy

January 2015
Volume 30 Number 1

Cover image courtesy of
Lee Pettet/Getty Images.

ON THE WEB

WEB SEMINARS

Assessing the Capability of Spectroscopy Techniques to Evaluate Water Quality
Tarun Anumol, The Snyder Research Lab at the University of Arizona

USP <232> and <233> Validation Protocol in Your Methods
Jonathan Sims, Tim Cuff, and Aaron Hineman, PerkinElmer

Single-Particle ICP-MS and Its Advantages in Analyzing Nanoparticles in Environmental Matrices
James Ranville, Colorado School of Mines; Kevin Wilkinson, Université de Montréal; and Chady Stephan, PerkinElmer, Inc.

Demystifying Interference Removal
Matthew Cassap and Christoph Wehe, Thermo Fisher Scientific

Add Isotope Ratio Information to Your Research
Andreas Hilkert, Thermo Fisher Scientific
spectroscopyonline.com/WebSeminar

Like *Spectroscopy* on Facebook:
www.facebook.com/SpectroscopyMagazine

Follow *Spectroscopy* on Twitter:
https://twitter.com/spectroscopyMag

Join the *Spectroscopy* Group on LinkedIn
http://linkd.in/SpecGroup

COLUMNS

Why Spectral Interpretation Needs To Be Taught
The first installment of this new column series explains why information on how to interpret infrared spectra is important, discusses some basic IR theory, and lays out a blueprint for future installments.
Brian C. Smith

Down to Earth: Measurements of Geological, Coal, and Soil Samples with LIBS
This article explores the use of laser-induced breakdown spectroscopy (LIBS) for measurements of elemental concentrations and bulk properties of heterogeneous, earthen-based samples.
Steve Buckley

Next-Generation Infrared Spectroscopic Imaging
Infrared spectroscopic imaging has been advancing significantly in recent years. Key to that advance is improving the understanding of the underlying mechanisms that influence the ability to achieve greater resolution and speed. Rohit Bhargava of the University of Illinois, Urbana-Champaign, recently spoke to *Spectroscopy* about his work elucidating those mechanisms. Bhargava won the 2014 Applied Spectroscopy William F. Meggers Award for his paper on this topic.

PEER-REVIEWED ARTICLE

A method for the multielemental determination of metals and nonmetals in goji berries by axially and radially viewed inductively coupled plasma–optical emission spectrometry (ICP-OES) is presented.
Angerson Nogueira Nascimento, Daniel Menezes Silvestre, Flávio de Oliveira Leme, Cassiana Seimi Nomura, and Juliana Naozuka

FEATURED ARTICLE

A review of the essential elements of MS approaches to protein quantification and a critical comparison of the available options
Mark W. Duncan, Alfred L. Yergey, and P. Jane Gale

DEPARTMENTS

Editorial Advisory Board

News Spectrum

Nominations Sought for AOAC Awards

AOAC International is seeking nominations for the Harvey W. Wiley Award and for recognition as a Fellow of AOAC International. The AOAC Awards Program recognizes significant contributions to the analytical science community and to AOAC itself.

The Harvey W. Wiley Award is presented to a scientist (or group of scientists) who has made an outstanding contribution to analytical method development in an area of interest to AOAC International. The recipient is selected from nominations received from members of the analytical science community, with nominations accepted year round. All nominating materials for the 2016 Harvey W. Wiley Awards must be received no later than January 31, 2015.

The Fellow of AOAC International Award recognizes meritorious service to the Association. This award is given to members of AOAC whose volunteer efforts have significantly contributed to the success and prestige of the Association. All nominating materials for 2015 Fellows of AOAC must be received no later than February 15, 2015.

For eligibility and nomination guidelines, visit the AOAC web site or contact May Rose Jones, Program Manager, at (301) 924-7077, ext. 114, or email at mjones@aoac.org.

SERS Assay Detects Anthrax Spores in 15 Min

A surface-enhanced Raman spectroscopy (SERS) assay that was designed to detect *Bacillus anthracis* spores was used to selectively bind *B. anthracis* with a 100-fold selectivity versus *B. cereus* and to detect *B. anthracis* Ames at concentrations of 1000 spores per milliliter within 15 min. The assay consisted of silver nanoparticles embedded in a porous glass structure functionalized with peptides distributed throughout a porous glass structure so that sample and reagents can easily flow through.

In a paper titled "Selective Detection of 1000 *B. anthracis* Spores Within 15 Minutes Using a Peptide Functionalized SERS Assay," published in the December issue of *Analyst,* researchers determined that the SERS assay measurements provide a basis for the development of systems that can detect spores collected from the air or from water supplies.

In their paper, authors Stuart Farquharson, Chetan Shende, Wayne Smith, Hermes Huang, Frank Inscore, Atanu Sengupta, Jay Sperry, Todd Sickler, Amber Prugh, and Jason Guicheteau note that "since the distribution of *B. anthracis* Ames spores through the US Postal System in 2001, there has been substantial effort to develop technologies that can detect this bioweapon as part of an early warning system." They conclude that the sensitivity of their SERS assay suggests that an early warning system capable of detecting the required 10^4 *B anthracis* Ames spores per cubic meter in ~10 min could be developed. They note that similar peptide-based SERS assays could be developed for food and waterborne pathogens, provided that the selective peptides and appropriate biomarkers are available. ∎

IS THERE AN APP FOR THAT?

HIGHLIGHTS OF APPS FOR SPECTROSCOPY

APP NAME: SpectrumLITE

OFFERED BY: ProjectLITE

PLATFORMS: iPhone, iPad, iPod touch (requires iOS 3.1 or later)

WHAT IT DOES: The SpectrumLITE app is designed for the display of the spectrum of light that can be emitted by the iPod or iPhone screen. According to the company, users can select a color from the diagram and a line of color will appear. The width of the line reportedly can be varied by tapping the screen and selecting pixel width using the slider. The spectral line can be viewed using either a prism or a diffraction grating.

COST: Free
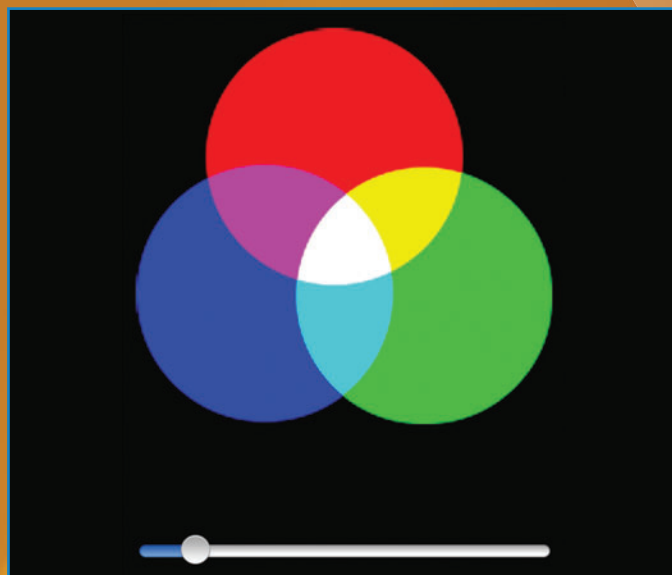
From the Editor

A Matter of Interpretation

Laura Bush is the editorial director of *LCGC North America* and *Spectroscopy*, lbush@advanstar.com.

Today, many practitioners of spectroscopic methods, particularly those working in industry, find themselves facing significant challenges. More and more often they are asked (read "required") — because of expanding work or decreased staffing — to take on the use of new techniques for which they do not have a strong background or training. To make matters worse, the use of the unfamiliar methods is being added to their existing workload, so they don't have much time to dedicate to learning how to use them. To top it off, the in-house "go-to person" — the highly experienced and highly educated expert from whom one could get help when dealing with a vexing problem — probably no longer exists within the company.

An additional complication in such situations is the old saying that "you don't know what you don't know." This problem very often arises in the interpretation of infrared spectra.

Inexperienced IR users sometimes think that interpreting spectra is simply a process of looking them up in some reference source. That approach, however, can often lead to errors — of which the user may not even be aware.

It is these concerns that have led us to launch a new quarterly column in *Spectroscopy*, called "IR Spectral Interpretation Workshop." In this new column, Brian C. Smith will explain the processes to interpret infrared spectra properly and thus help readers interpret the spectra of important functional groups. To provide the right foundation for those explanations, he will start by laying out some basic theory of infrared spectra.

Brian spent more than 20 years training spectroscopists, so he knows first hand the challenges you face as you learn and become more expert in these methods. He has written three books on the subject, so he also knows how to explain the concepts in writing.

Check out Brian's first installment in this issue. I think you will find his explanations extremely clear and enlightening. In future installments, he will provide examples of spectra for readers to interpret on their own, with answers being revealed in subsequent issues. During your work on those problems, you can also contact Brian for help and clarification of doubts you faced along the way.

We hope you enjoy this new column, and that you participate in the interactive elements of it too.

Laura Bush

X-Ray Detectors

- **Solid-State-Design**   - **Low Cost**   - **Easy to Use**

The PERFORMANCE You Need

SDD

125 eV FWHM

5.9 keV

^{55}Fe

25 mm^2 x 500 μm
11.2 μs peaking time
P/B Ratio: 20000/1

Energy (keV)

Si-PIN

145 eV FWHM

5.9 keV

^{55}Fe

6 mm^2 x 500 μm
25.6 μs peaking time
P/B Ratio: 6200/1

Counts

Energy (keV)
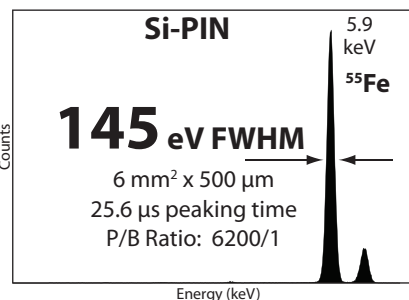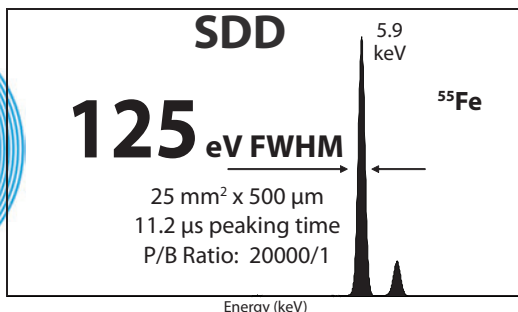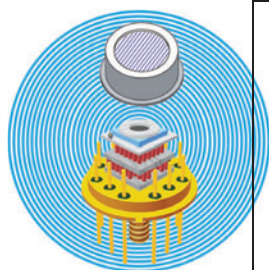
FAST SDD®

Count Rate = >1,000,000 CPS

Resolution	125 eV FWHM	130 eV FWHM	140 eV FWHM	160 eV FWHM
Peaking Time	4 μs	1 μs	0.2 μs	0.05 μs

Resolution vs Peaking Time

25 mm^2

Standard SDD

FAST SDD®

Resolution (eV FWHM @ 5.9 keV)

Peaking Time (μs)

Throughput

0.2 μs

1 μs

4 μs

Output Count Rate (OCR)

Input Count Rate (ICR)
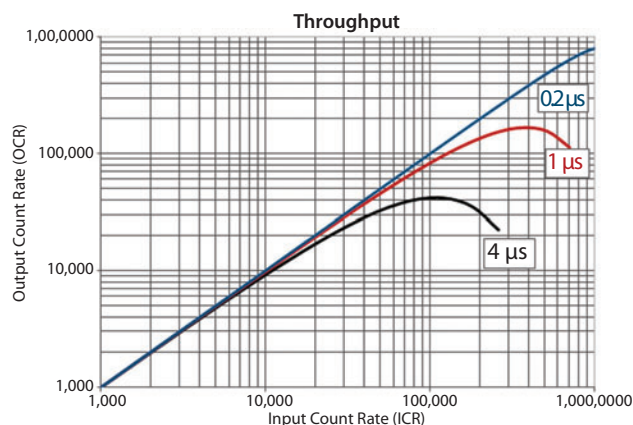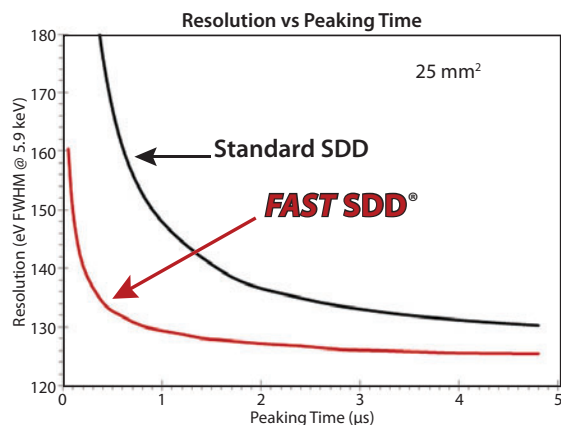
The CONFIGURATION You Want

XRF Experimenter's Kit

X-Ray Spectrometer

OEM Components for XRF

XRF System

OEM's #1 Choice for XRF
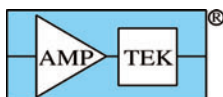
AMPTEK Inc.
www.amptek.com

AMPTEK®

AMETEK®
MATERIALS ANALYSIS DIVISION
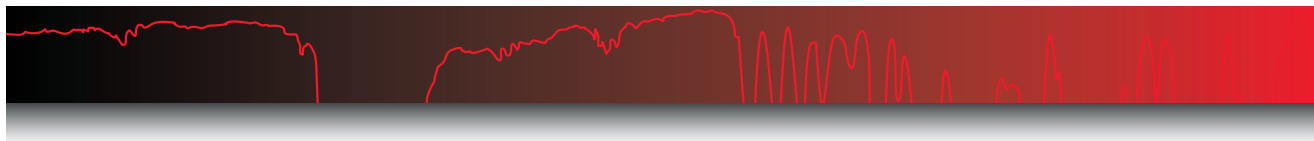
IR Spectral Interpretation Workshop

Why Spectral Interpretation Needs To Be Taught

There is a continuing need for Fourier transform infrared (FT-IR) users to receive training in how to interpret the infrared spectra they measure. This new column will provide practical advice about how to do this. This first installment will present why this type of column is important, discuss some basic IR theory, and lay out a blueprint for future installments.

Brian C. Smith

Infrared (IR) spectroscopy is widely used to determine the structures of unknown molecules, give a fingerprint of a sample, and measure the concentrations of molecules in samples (1–4). When a molecule absorbs infrared light, it undergoes a spectroscopic transition from a lower to an upper vibrational energy level, as seen in Figure 1.

The absorbed infrared energy causes the molecule's bonds to stretch and bend. In most cases, these vibrations are localized to specific portions of a molecule called *functional groups*. Examples of functional groups include the methyl group (CH_3–), the carbonyl group (C=O), and benzene rings (C_6H_6).

The *x*-axes of most infrared spectra are plotted in wavenumber (cm^{-1}) units. The wavenumber of electromagnetic radiation is proportional to energy (1). When infrared light of the same energy as a vibrational transition impinges upon a molecule, the energy may be absorbed. The corresponding decrease in light energy at the absorption wavenumber gives rise to a peak in the measured infrared spectrum of the molecule. The peak positions in an infrared spectrum thus disclose the vibrational energy levels of the functional groups in a molecule, and when infrared spectra are analyzed, the peaks are assigned to specific vibrations of specific functional groups. Thus, infrared spectroscopy is a type of functional group spectroscopy, and infrared spectrometers are used to detect functional groups. The peak positions in an infrared spectrum are used to distinguish different functional groups from each other.

Different functional groups can have peaks at about the same position. For example, both O–H and N–H stretches have peaks around 3350 cm^{-1} (4). In these cases, how can one distinguish the peaks of different functional groups from each other? The answer is that in addition to peak position information, infrared spectra contain peak heights and peak widths. Different functional groups have different peak intensities and peak widths. For example, one can distinguish O–H and N–H stretches from each other because normally O–H stretching peaks are more intense and broader than N–H stretching peaks. By integrating the peak position, height, and width information in a spectrum you will be more successful at interpreting spectra than just using the peak positions by themselves. The purpose of this installment is to teach why different functional groups have different peak positions, heights, and widths so that infrared interpreters can integrate this information to more readily distinguish different functional groups from each other.
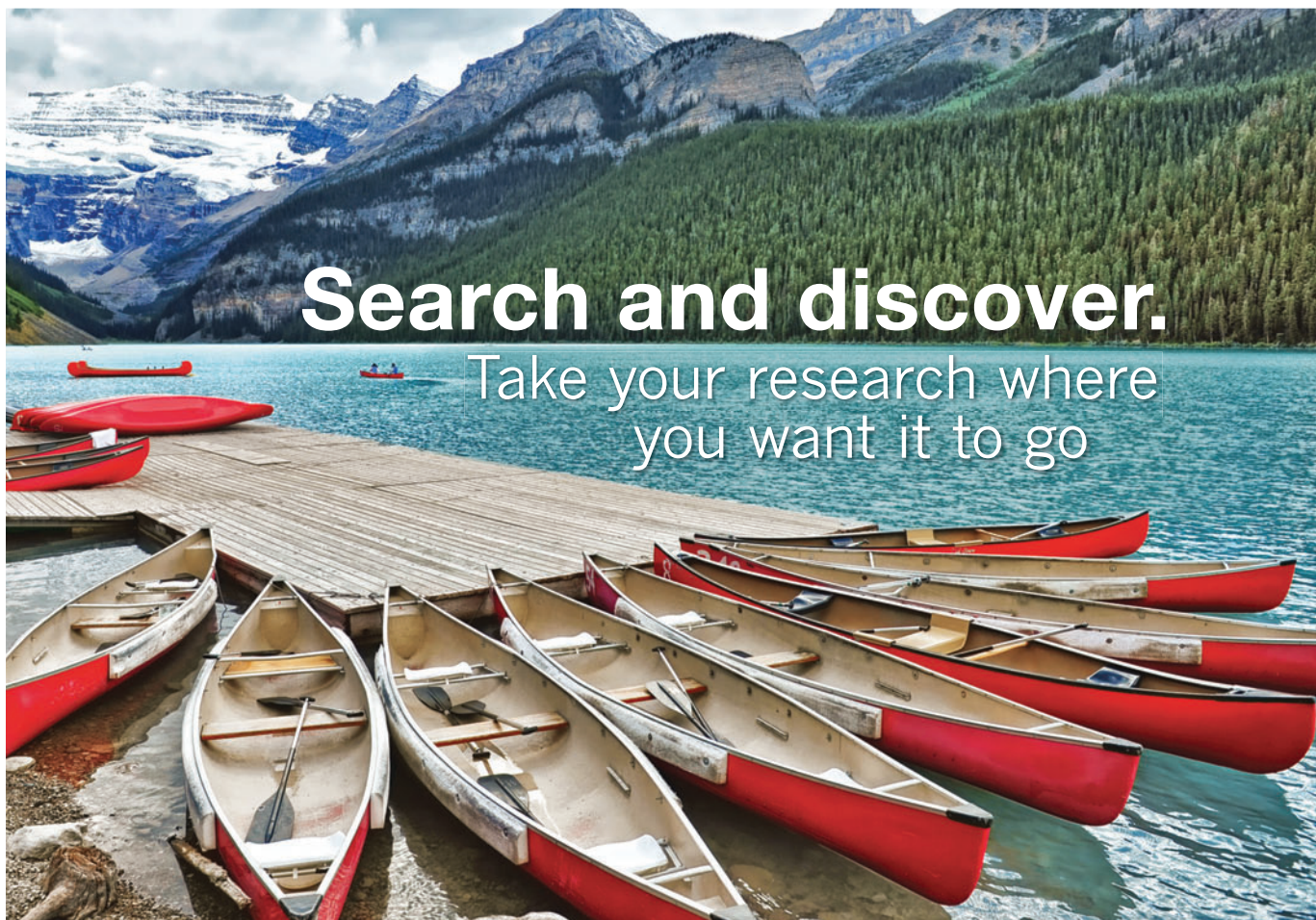
Search and discover.
Take your research where you want it to go

Introducing the new website from Harrick Scientific, pioneer of IR and UV-Vis sampling techniques, industry innovator for over 40 years. **www.harricksci.com**

Our new website was designed to assist you through any spectroscopy challenge. Harrick Scientific offers a comprehensive array of sampling tools for a wide range of applications, from routine quality control to advanced research investigations. **Harrick accessories extend the capabilities of FTIR and UV-Vis spectrometers to perform analyses that would otherwise be difficult or impossible.**

Through our site you'll gain guided access to application solutions, plus technical information, application notes and references. We also offer a full range of consumables and optics for online purchase. Our site is backed by a team of scientists, engineers, and industry experts. **In other words, the perfect place to turn to when embarking on your next endeavor.**

Visit our website for details about our newest addition, the Video MVP.
www.harricksci.com/Introducing-VideoMVP

HARRICK **Scientific Products**

141 TOMPKINS AVE P.O. BOX 277 PLEASANTVILLE, NEW YORK 10570 T 914-747-7202 F 914-747-7209 INFO@HARRICKSCI.COM
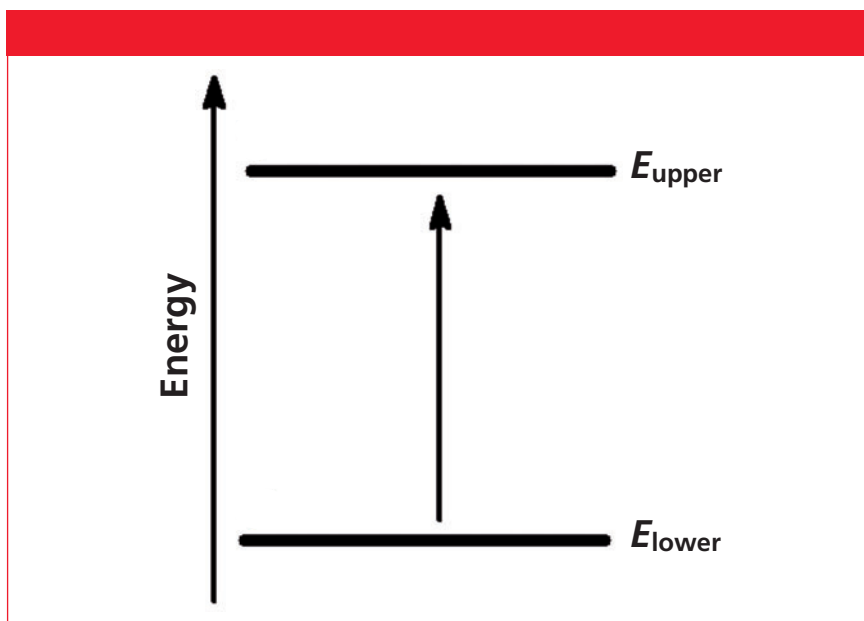
Figure 1: A spectroscopic transition occurs when infrared light is absorbed by a molecule and it is excited from a lower to an upper vibrational energy level.
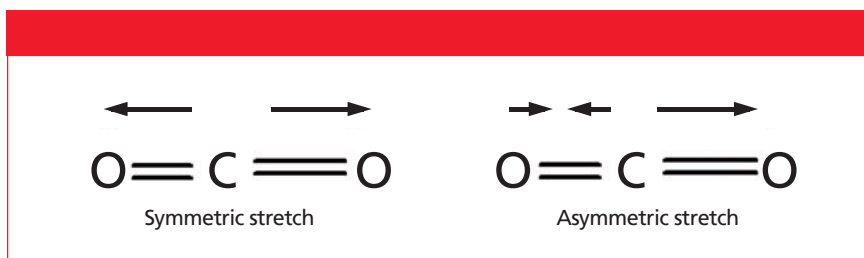
Figure 2: Left: the symmetric stretch normal mode of the carbon dioxide molecule. Right: the asymmetric stretch normal mode of the same molecule. The arrows note the displacement of the oxygen atoms during the vibrations.
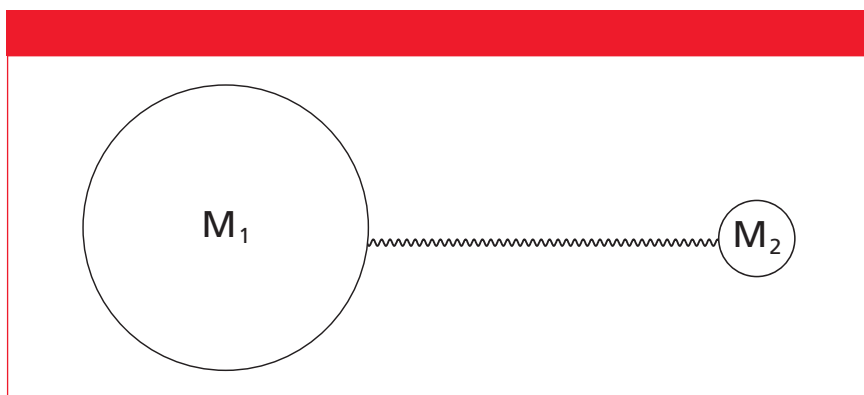
Figure 3: The ball-and-spring model for a generic diatomic molecule containing atoms of masses M_1 and M_2.

Peak Positions

Given that the absorption of infrared light excites molecular vibrations, we need to understand these vibrations to make sense of infrared spectra. The constituent vibrations of a molecule (or any physical object for that matter) are referred to as its *normal modes* (4–7). An illustration of the symmetric and asymmetric stretching normal modes of carbon dioxide is seen in Figure 2.

At equilibrium CO_2 is symmetrical and both C=O bonds are the same length. During the symmetric stretch vibration the two oxygen atoms move in opposite directions, and at all points during the vibration the two C=O bonds have the same length, thus preserving the symmetry of the molecule. On the other hand, during the asymmetric stretch vibration the two oxygen atoms move in different directions, the bond lengths differ from each other, and the symmetry of the molecule is broken. To understand the relationship between molecular vibrations and peak positions it is easiest to begin by considering the generic diatomic molecule seen in Figure 3.

Shown is a ball-and-spring model where individual atoms are represented by balls and chemicals bonds by springs. The atoms in Figure 3 have masses M_1 and M_2, respectively. A real world example of such a molecule would be hydrogen chloride, H–Cl, where atom 1 would correspond to chlorine and atom 2 to hydrogen.

Diatomic molecules have only one vibration (4), the stretching of the single chemical bond, and hence have only one vibrational peak. Our goal is to derive an equation that will tell us the wavenumber of the vibrational peak in the spectrum of a diatomic molecule. To solve this problem we have to apply some physics to the matter. We define the reduced mass of our diatomic molecule as such:

$$M_R = (M_1 M_2)/(M_1 + M_2) \qquad [1]$$

where M_R is the reduced mass, M_1 is the mass of atom 1, and M_2 is the mass of atom 2.

By using a single quantity to represent the mass of this two-mass system, the mathematics of the derivation is made easier. The second piece of physics we have to consider is Hooke's law (4), which describes the behavior of springs (and chemical bonds) as such:

$$F = -kx \qquad [2]$$

where F is the restoring force of the

spring, k is the force constant of the spring, and x is the distance the spring is stretched.

Anyone who has ever stretched a rubber band has an intuitive grasp of Hooke's law. F is the amount of force needed to stretch and maintain the rubber band at a given length and is equal to the amount of force the rubber band is putting on the person trying to stretch it (the restoring force). Experience shows that it takes more force to stretch a rubber band a long distance than a short distance, which is why the variable x appears in Hooke's law. Experience also shows that it takes more force to stretch a stiff rubber band than a weak one, which is why the force constant appears in Hooke's law.

If one takes the reduced mass, Hooke's law, applies one of Newton's laws, and solves the resulting differential equation, this result is obtained (4):

$$W = (1/2\pi c)(k/M_R)^{1/2} \qquad [3]$$

where W is the peak wavenumber position in cm^{-1}, c is the speed of light, k is the force constant, and M_R is the reduced mass.

Equation 3 predicts the position in wavenumbers of the single vibrational peak for the generic diatomic molecule seen in Figure 3. This peak position is determined by the force constant, hence the strength of the molecule's chemical bond, and the mass of the two atoms composing the bond. Since k is in the numerator, as the force constant goes up the peak position increases. This means strong chemical bonds have higher peak positions than weak chemical bonds. The denominator in equation 3 contains the reduced mass, thus molecules with heavy atoms in them have lower wavenumber peaks than molecules with light atoms in them.

If two molecules have different chemical structures, they will have different force constants, reduced masses, and hence different infrared spectra. Put another way, a molecule's infrared spectrum truly is its chemical fingerprint, and it is as unique to it as your

DNA is to you. Of course, not all molecules are diatomic, and not all functional groups contain just two atoms. However, the ideas summarized in equation 3 are generally applicable to the functional groups in any molecule.

Infrared spectra have been measured for over a century (8). In this time, perhaps millions of samples have been analyzed, giving us a vast database of peak positions for known functional groups. This database has allowed the development of tables and charts noting the peak positions corresponding to specific functional groups (4–7). These tables are used to interpret the spectra of unknown samples and determine the functional groups present. Equation 3 thus explains why different functional groups have different peak positions.

Peak Heights

When plotted in absorbance units, the peak heights in an infrared spectrum are proportional to concentra-

Figure 4: The dipole moments of the CO_2 molecule. Partial positive and negative charges are represented by lower case deltas. Dipole moment vectors are represented by arrows.
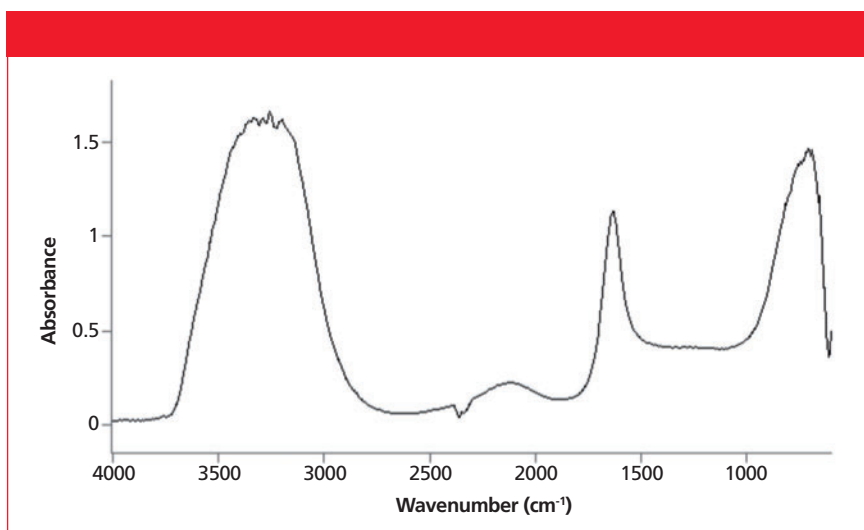
Figure 5: The infrared spectrum of liquid water. The O–H stretching peak centered near 3300 cm⁻¹ has a full width half maximum of about 500 cm⁻¹.
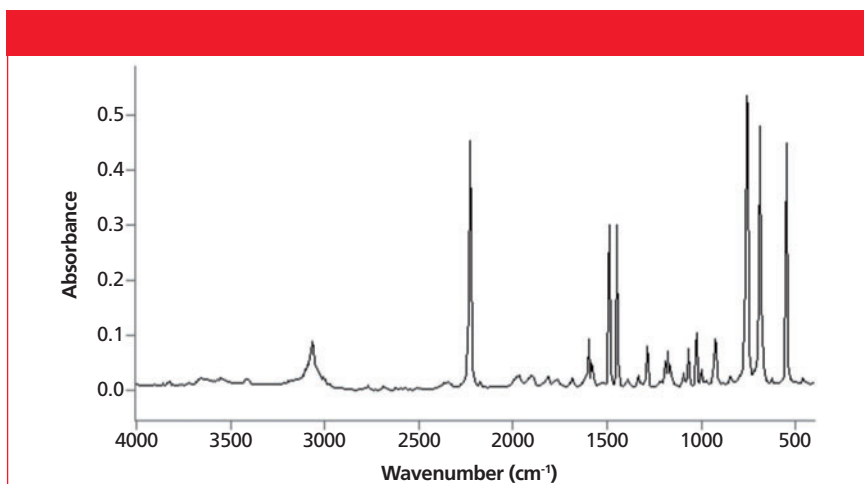
Figure 6: The infrared spectrum of benzonitrile. Note the narrowness of the peaks.

tion, allowing infrared spectra to be used to determine the concentration of chemical species in samples. The relationship between absorbance and concentration is summarized in Beer's law (consult reference 3 for the assumptions behind the deriva-tion of this equation):

$$A = \varepsilon l c \qquad [4]$$

where A is the absorbance, ε is the absorptivity, l is the pathlength, and c is the concentration.

The pathlength is simply the thickness of sample seen by the in-frared beam. Nominally, the absorptivity is the proportionality constant between absorbance and concentration. The absorptivity is also a phys-ical constant for a given pure mol-ecule at a given wavenumber, which means absorptivity must be related to a molecule's chemical structure. To understand this connection we must first understand the concept of dipole moments, which is illustrated in Figure 4.

In CO_2 the electronegativity dif-ference between the carbon and the oxygen atoms causes the electrons to be shared unevenly, leading to a partial positive charge on the carbon and negative charges on the oxygens. In Figure 4 the partial charges are represented by low-ercase deltas. A dipole moment is simply two charges separated by a distance, so each of the bonds in CO_2 has a dipole moment called a *bond dipole.* The dipole moment is a vector quantity, having both a magnitude and a direction. The length of the arrows in Figure 4 de-notes the magnitude of each bond dipole, and the arrows represent their direction. A bond's dipole moment is equal to the size of the charges in a bond times the dis-tance they are held apart as such:

$$\mu = qr \qquad [5]$$

where μ is the dipole moment, q is the charge, and r is the distance. (Please note: In physics the Greek letter μ is used to represent both re-duced mass and dipole moment. To avoid confusion in these columns μ will always represent dipole moment, and M_R will represent reduced mass.)

Thus, the dipole moment is a measure of charge asymmetry. Polar bonds such as O–H and C=O have large charge asymmetry and hence large dipole moments. Cova-lent bonds like C–C single bonds have little charge separation and hence small dipole moments.

The net dipole moment for a molecule is the sum of the bond

dipoles for that molecule. For a CO_2 molecule at equilibrium the net dipole is zero because the two bond dipoles are equal in magnitude and point in opposite directions, thus canceling each other. When the CO_2 molecule stretches symmetrically, as seen in Figure 2, the symmetry of the molecule is maintained and the two C=O bond dipoles are at all times still equal in magnitude and opposite in direction. As a result, the change in dipole moment, $d\mu$, with respect to bond length, dx, for the symmetric stretch of CO_2 is zero. In other words

$$d\mu/dx = 0 \qquad [6]$$

A close examination of the infrared spectrum of carbon dioxide shows that the intensity for this peak is zero, that is, there is no peak in the spectrum of CO_2 assignable to this vibration.

On the other hand, when CO_2 stretches asymmetrically, as seen in Figure 2, the symmetry of the molecule is broken, the bond dipoles no longer cancel at all points during the vibration, and there is a large change in dipole moment with respect to bond length during the vibration. In other words

$$d\mu/dx \neq 0 \qquad [7]$$

The corresponding peak in the molecule's infrared spectrum falls around 2350 cm^{-1} and is quite intense. This peak is sometimes seen in sample spectra measured with a Fourier transform infrared (FT-IR) spectrometer.

Thus, there is a connection between $d\mu/dx$ and intensity, but how does this new discovery of ours fit in with Beer's law? I will skip the derivation here, but quantum mechanics tells us that (3,9)

$$\varepsilon = (d\mu/dx)^2 \qquad [8]$$

where ε is the absorptivity, $d\mu$ is the change in dipole moment during a vibration, and dx is the change in bond length during a vibration.

Thus, the absorptivity, which is a fundamental constant for a pure molecule at a given wavenumber of
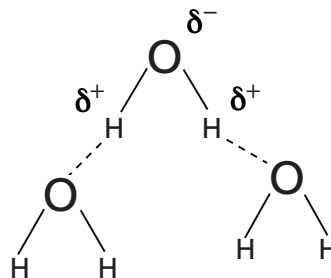
Figure 7: An illustration of the hydrogen bonding that takes place in liquid water.

absorption under standard conditions, depends on the electronic structure of a molecule and how it changes during a vibration. Polar functional groups will have large dipole moments, will frequently have vibrations for which $d\mu/dx$ is large, and will have intense peaks. Nonpolar functional groups will have small dipole moments, will frequently have vibrations for which $d\mu/dx$ is small, and will have infrared features that are weak or even nonexistent. This means that infrared spectroscopy is better at detecting some functional groups than others, and that polar functional groups are generally the easiest to detect. Equation 6 shows why different functional groups have different peak intensities.

Peak Widths

Infrared peak widths vary greatly across the spectrum of known molecules. Figure 5 shows the infrared spectrum of liquid water. The full width half maximum (FWHM) of the O–H stretching peak at 3300 cm^{-1} is about 500 cm^{-1}. This is an unusually broad peak for an infrared spectrum. Figure 6 shows the infrared spectrum of the organic molecule benzonitrile. In this spectrum the FWHMs are less than 50 cm^{-1}. There is an order of magnitude difference in peak width between these two spectra, but why? The answer lies in the strength of the intermolecular interactions for the two compounds. Water engages in hydrogen bonding, as seen in Figure 7, which is a strong type of intermolecular interaction.

When intermolecular interactions are strong, the strength of the intermolecular bonds varies over a wide range, giving rise to a large number of energy states. Each of these states will absorb infrared light at a number of slightly different wavenumbers, giving rise to broad peaks. The intermolecular interactions in benzonitrile are weak because they are due to van der Waals forces, the corresponding number of energy states is small, infrared light is absorbed at a small number of wavenumbers, and hence the peak widths are narrow.

In general, functional groups that have strong intermolecular interactions will have broad peaks. For example, most molecules containing the O–H functional group engage in hydrogen bonding and have broad peaks. Functional groups that have weak intermolecular interactions such as aromatic rings will generally have narrow peaks. It is the varying strengths of intermolecular interactions that cause different functional groups to have different peak widths.

Conclusion

Infrared spectroscopy is used to detect functional groups in samples. Infrared spectra contain information about peak position, height, and width. Peak positions are determined by the force constants and reduced masses

of a vibrating functional group. Peak heights are determined by Beer's law, including absorptivity, pathlength, and concentration. Absorptivity depends upon (dμ/dx)^2 for a given vibration of a given functional group. Peak widths are determined by the strength of intermolecular interactions in a sample. All of these pieces of information need to be understood and integrated properly to successfully distinguish the spectra of different functional groups from each other.

References

(1) B.C. Smith, *Fundamentals of Fourier Transform Infrared Spectroscopy, 2nd Edition* (CRC Press, Boca Raton, Florida, 2011).
(2) P. Griffiths and J. de Haseth, *Fourier Transform Infrared Spectrometry, 2nd Edition* (Wiley, New York, New York, 2007).
(3) B.C. Smith, *Quantitative Spectroscopy: Theory and Practice* (Academic Press, Boston, Massachusetts, 2002).
(4) B.C. Smith, *Infrared Spectral Interpretation: A Systematic Approach* (CRC Press, Boca Raton, Florida, 1999).
(5) N. Colthup, L. Daly, and S. Wiberley, *Introduction to Infrared and Raman Spectroscopy* (Academic Press, Boston, Massachusetts, 1990).
(6) D. Lin-Vien, N. Colthup, W. Fateley, and J. Graselli, *The Handbook of Infrared and Raman Characteristic Frequencies of Organic Molecules* (Academic Press, Boston, Massachusetts, 1991).
(7) G. Socrates, *Infrared and Raman Characteristic Group Frequencies: Tables and Charts* (Wiley, Boston, Massachusetts, 2001).
(8) W. Coblentz, *Phys. Rev.* **16,** 35 (1903).
(9) J.M. Hollas, *Modern Spectroscopy 3rd Edition* (Wiley, New York, New York, 1996).

For more information on this topic, please visit our homepage at: www.spectroscopyonline.com

Brian C. Smith, PhD, is a Senior Infrared Product Specialist for PerkinElmer, based in San Jose, California. Before joining PerkinElmer, he ran his own FT-IR training and consulting business for more than 20 years, and taught thousands of people around the world how to improve their FT-IR analyses and interpret infrared spectra. Dr. Smith has written three books on infrared spectroscopy: *Fundamentals of FTIR* and *Infrared Spectral Interpretation,* both published by CRC Press, and *Quantitative Spectroscopy: Theory and Practice* published by Academic Press. He has published a number of papers in peer-reviewed journals and is a co-inventor on a patent for an FT-IR method to monitor dust exposure in coal mines. Earlier in his career, Dr. Smith worked as a spectroscopy applications specialist at Princeton Instruments and Digilab, and as a research chemist at AT&T Bell Labs, IBM, and Xerox. Dr. Smith earned his PhD in Physical Chemistry from Dartmouth College.

Lasers and Optics Interface

Down to Earth: Measurements of Geological, Coal, and Soil Samples with LIBS

This article explores the use of laser-induced breakdown spectroscopy (LIBS) for measurements of elemental concentrations and bulk properties of heterogeneous, earthen-based samples. Rapid field and industrial measurements of these matrices are difficult using traditional methods. Here, we discuss the progress and promise of LIBS in making these measurements. Sample preparation, calibration, and typical results are shown. Of particular interest is the ability to extract physical properties from LIBS measurements. Examples such as heating value and volatile matter of coal, directly derived from LIBS spectra, show the ability and potential of the method to be used in fielded industrial measurements for rapid decision-making.

Steve Buckley

Avariety of basic industrial and energy-related procedures involve processing large quantities of geologically derived material. Examples include exploration and production geology in the oil and gas industry, mining of phosphates for the fertilizer industry, coal mining, and cement production. Similar needs exist in agriculture for the evaluation of soil macronutrients such as potassium and phosphorus before the application of fertilizers. In these cases, composition analysis can directly yield concentrations of interest (for example, phosphate in mined rock or potassium in soil), a suite of elements can provide in-

formation used to guide operations (such as characterization of geology during drilling), and models based on composition measurements can directly yield properties of geologically derived material (for example, total ash content or heating value of coal).

Each of these high-throughput processing environments would benefit from more immediate data that could be linked directly to guide processing. Real-time data with closed-loop feedback is the ultimate goal in each case. Benefits, projected or already realized, include increasing mining recovery, improving oil and gas exploration and recovery, precision blend-

Figure 1: Typical sample press. There is a die between the platens and extra dies to the right of the press.

Figure 2: Pressed soil pellet ready for analysis.

Figure 3: Schematic layout of the integrated LIBS analyzer.
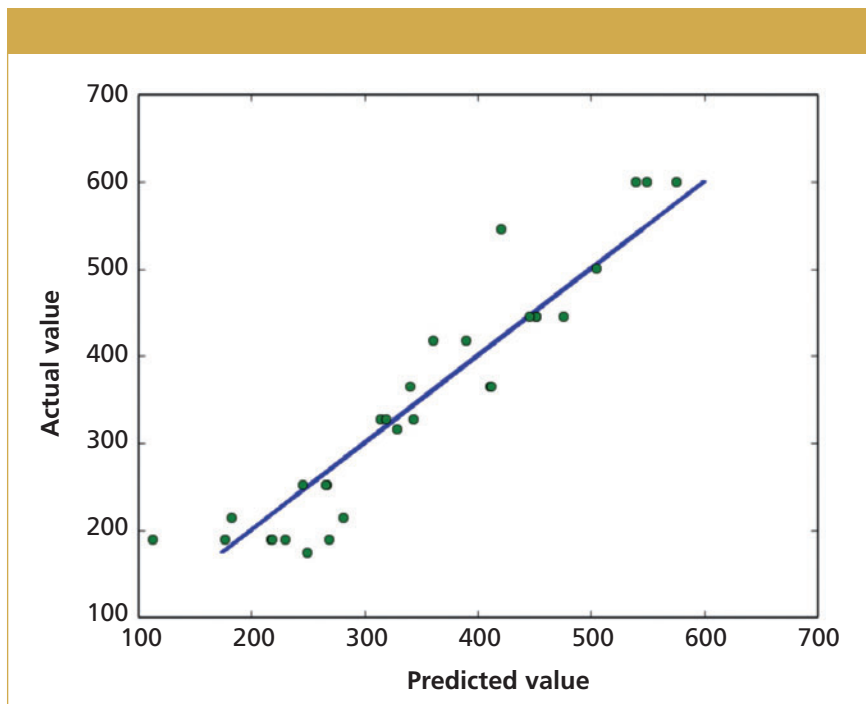
Figure 4: Prediction of potassium in soil from a very limited dataset. For the predicted value: explained variance = 89%, mean error = 34.

ing of mined components to optimize product streams, data-driven application of fertilizer to reduce waste and enhance agricultural productivity, and efficient operation of coal power plants. In each of these cases, the analysis step is typically a bottleneck. Traditional laboratory-based analysis yields high precision and accuracy, but with a significant time penalty. One of the opportunities for laser-induced breakdown spectroscopy (LIBS) technology is to exploit the ability for remote or stand-off real-time analysis to improve the speed of the analysis process, moving these operations closer to closed-loop control.

LIBS Capabilities

Several recent tutorial articles in this magazine (1–3) as well as a number of monographs (4,5) and a burgeoning amount of applications-based literature provide

This diversity of spectra thus obtained presents challenges for LIBS. One of these challenges is that the absolute signal for the specific component being measured in this "unmixed" manner is much greater than it would be if the sample were homogenous.

background on the capabilities of LIBS analysis and suggestions for hardware configurations. The stand-off projection of the laser onto the sample and the rapid analysis capabilities are key attributes of LIBS for earthen-based samples, as well as the ability to measure light elements. In addition, full-spectrum analysis can be used for direct correlation of spectra to properties, avoiding the need to measure every element and subsequently model properties.

There are numerous commonalities between soil, coal, and geological sample analyses. Each sample type is a heterogeneous material requiring bulk analysis. There are multiple important major elements (such as N, P, and K in soil and C and H in coal), and the range of important trace elements is between approximately 10–500 ppm. These measurement requirements are within LIBS detection limits, and the precision needs are also within the reach of LIBS technology, between 1–3% relative error over the bulk of the analysis range. Each of the measurements also can benefit from the ability to analyze light elements such as C, H, and N.

Sample Handling

There are two options for obtaining a representative set of LIBS spectra from heterogeneous materials for analysis. The first is to acquire and average many shots on the heterogeneous sample, forming a composite spectrum (or set of spectra) that can subsequently be used for quantification. In a truly heterogeneous sample with a heterogeneity scale on the order of the analysis spot size, each laser shot hits a distinct type of inclusion in the bulk. This condition is close to true for earthen-derived samples. Hence, some laser shots could, for example, hit mineral inclusions of SiO_2, others could hit $CaCO_3$, and still others could hit organic matter, and so on. The question is: Can a set of heterogeneous spectra be used to easily quantify elements, classify types of materials, or determine properties?

This diversity of spectra thus obtained presents a pair of related challenges for LIBS. One challenge is that

Figure 5: Volatile matter in coal (percent), predicted by LIBS versus actual.

Figure 6: Heating value of coal (MJ/kg, dry), predicted by LIBS versus actual.

mixed throughout the sample. Such wide signal variation would put a requirement for dynamic range on the detector that would be difficult or impossible to meet in practice. A second challenge is that calibration becomes much harder in the unmixed state. Because LIBS calibrations are matrix-dependent, using a single calibration depends on having a homogenous, known matrix. A calibration cannot be easily performed on the "average" spectrum because the intensities of each line are not only dependent on the underlying elemental concentration, but also on the overall composition of the material. Therefore, in this case, it is likely that independent calibrations of the types of minerals in the "unmixed" materials would be required to obtain accurate calibrations. Alternatively, calibrations could be built based on composite spectra, but such calibrations would be quite sensitive to the specific mineralogy of each element in the sample, as that mineralogy would form the "matrix" for each element. In contrast, in a truly homogenous sample, the large part of the matrix remains the same in each spectrum.

Homogenizing the sample is thus the easier approach, from a calibration and analysis standpoint. This can be done using a variety of methods. In the laboratory, samples are commonly ground and pressed in a pellet press with a known force for a particular period of time. Figure 1 shows a common sample press used in our laboratory. Sample is placed in the dies (examples shown on the right) and then pressed to up to 20 tons between the platens in the press. From experience, it is important to press the samples to uniform pressure and time to ensure that the LIBS ablation event remains the same for each analysis. Varying time and pressure in the preparation results in samples that ablate differently, and hence have unwanted spectral variations. Figure 2 illustrates a pellet pressed from a soil sample. The pellet is

the absolute signal for the specific component being measured in this "unmixed" manner is much greater than it would be if the sample were homogenous. For example, if 5% of a sample were MgO, and this were the primary form of Mg in the sample, we would expect that an unmixed sample would experience roughly 20 times the Mg signal when an inclusion of MgO were hit than if the MgO were crushed and thoroughly

hard (does not crumble) and has a slightly smaller diameter than a United States penny.

Analysis

All of the samples were tested in one of the ChemReveal integrated LIBS spectrometers in our laboratory at TSI. This is a Class-1 (eye-safe) integrated laboratory system with a basic layout shown in Figure 3. Samples inserted into the system are visualized on a video camera and spectra from single spots, lines, or grids of analysis spots can be obtained. No inert gas purge was used on any of the samples, although this is an option that can, in some cases, improve signal-to-noise ratios.

Soil, coal, and geological samples from drilling operations were all analyzed under different experimental conditions as part of ongoing studies. Examples are presented here to illustrate the range of possibilities. For example,
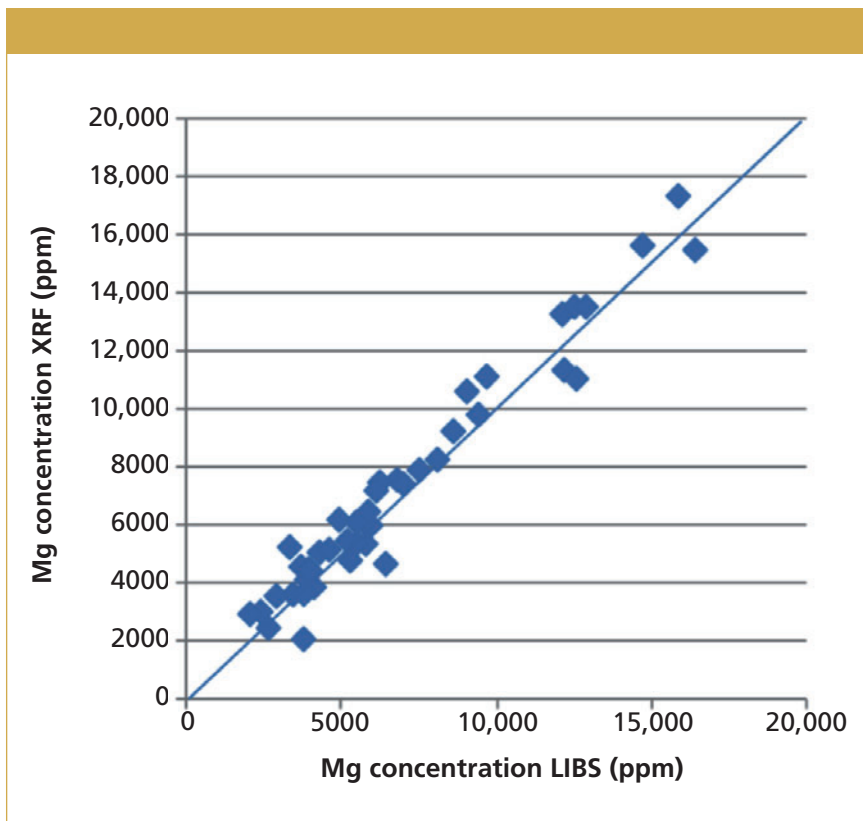
Figure 7: Magnesium concentration measured with LIBS versus XRF.

our partner company dickey-JOHN has a soil database of 500 well-characterized soils. From this, we obtained 15 samples with a range of characteristics to see how well we could correlate potassium concentrations. We pressed the samples as shown in Figure 2, and took a small number of LIBS spectra (160 individual spectra) by making 10 shots on a 4×4 grid on each sample. We focused 70-mJ pulse energy into 300-μm spots.

Spectra were averaged in groups of four, resulting in 40 spectra per individual sample. Data were fed into a support vector machines algorithm, with 95% of the overall data used for training the calibration model, and 5% of the data reserved for testing.

Figure 4 shows the results of this very preliminary study with a limited number of data points. Predicted potassium concentration (in inconvenient units of "lb/acre")

is shown on the *x*-axis and ICP measurements of the actual value are shown on the *y*-axis. The blue line is the model calibration and the green points are the prediction of the model using the independent test data. The model explains 89% of the variance in the data and the mean error is 34 units. In practice, far more data would be used to build such a model, but this initial validation has provided an impetus for further work in our laboratory.

An example in which much more data was used (with much better results, as shown) is in some recent coal measurements we accomplished with Tsinghua University. This study, with the group of Professor Zhe Wang, is part of a larger collaboration aimed at developing LIBS-based coal analyzers. Here, we have a database of more than 75 well-characterized coals that are commonly used in China, from which we have taken hundreds of spectra over time. We have used the data to build a predictive model for both elemental concentrations and numerous coal properties of interest in power plant operations. Examples of LIBS-based property predictions are shown in Figures 5 and 6. Actual measurements used for reference were Chinese standard methods performed in multiple laboratories. Figure 5 shows accurate prediction of volatile matter (in percent), while Figure 6 illustrates direct prediction of coal heating value (in MJ/kg) using LIBS. Recent on-site tests of the system at the Zhangqiu power plant owned by China Huadian Corporation has shown overall validation error of less than 1% for the system for several of the parameters of interest.

Similar to the coal work, a LIBS analysis of core samples from a drilling operation (energy exploration) was performed to determine elemental concentrations. As previously done, samples were ground and pressed into pellets. A partial least squares-based model was used to quantify concentrations from the
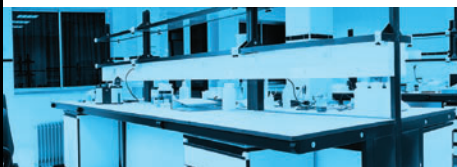
LIBS spectra, using X-ray fluorescence (XRF) measurements as the standard method. Example relative standard deviations for multiple elements shows the repeatability of the LIBS measurement to be between 2% and 6%. Figure 7 shows the results for Mg, which are representative of most of the elements tested. It is expected that the uncertainty in the XRF measurement is comparable if not greater than the uncertainty in the Mg measurement.

Implications

These measurements clearly indicate the potential for LIBS in measurements of earthen-based samples. Homogenizing the samples before measurement allows accurate and repeatable measurements, even in tough conditions, as shown in on-site measurements. Interestingly, LIBS can be used to measure elemental concentration, sample type, or sample properties directly. The exploratory work shown here has led to additional efforts in sampling and method automation that are quite exciting. The real-time analysis and light element capability of LIBS makes it clearly attractive for rapid laboratory and field measurements of geological materials of many kinds.

Acknowledgments

The author thanks Dr. Markus Gaelli (TSI) for generously taking the data on soil samples at short notice, and acknowledges Dr. Gregg Lithgow and Kregg Philpott (also both with TSI) for helping to acquire the data from the geological samples.

References

(1) S. Buckley, *Spectroscopy* **29**(1), 22–29 (2014).
(2) S. Buckley, *Spectroscopy* **29**(4), 26–31 (2014).
(3) S. Buckley, *Spectroscopy* **29**(10), 24–33 (2014).
(4) D.A. Cremers and L.J. Radziemski, *Handbook of Laser-Induced Breakdown Spectroscopy* (Wiley, Hoboken, New Jersey, 2013).
(5) R. Noll, *Laser-Induced Breakdown Spectroscopy: Fundamentals and Applications* (Springer, Heidelberg, Germany 2012).

Dr. Steve Buckley is Director of Market Development at TSI Incorporated, which acquired the LIBS business of Photon Machines, Inc. in 2012. Prior to cofounding Photon Machines, Steve was a tenured professor of engineering at the University of California, San Diego. He has been working on research and practical issues surrounding the implementation of LIBS since 1998. Steve can be reached at steve.buckley@tsi.com

For more information on this topic, please visit our homepage at: www.spectroscopyonline.com

Next-Generation Infrared Spectroscopic Imaging

Infrared spectroscopic imaging has been advancing significantly in recent years. Key to that advance is improving the understanding of the underlying mechanisms that influence the ability to achieve greater resolution and speed. Rohit Bhargava, a professor in the Department of Bioengineering and at the Beckman Institute at the University of Illinois, Urbana-Champaign, has been elucidating those mechanisms, and won the 2014 Applied Spectroscopy William F. Meggers Award for his paper on this topic. He recently spoke to *Spectroscopy* about this work.

In your recent paper on high-definition infrared spectroscopic imaging (1), you describe a model for light propagation through an infrared spectroscopic imaging system based on scalar wave theory. How does this approach differ from traditional approaches?

Bhargava: That's a great question. Traditionally, there have been two approaches. One is the so-called ray model approach, in which the wavelength of light is much smaller than the features of interest in your sample. Clearly that doesn't hold for microscopically diverse samples in an infrared microscope where you're trying to look at feature sizes of 10–15 μm or smaller with wavelengths of light that have approximately the same dimensions. In 2010, we published a series of papers describing the electromagnetic model, which is a fully detailed model that accounts for light propagation explicitly with structures that is fully accurate from first principles. This model is also computationally very, very intensive, so doing large-scale modeling with that type of approach is difficult. The new approach that we've proposed in this paper is actually a happy medium. It provides a very high level of detail so that you can capture the right physics but it's also computationally very tractable so you can actually start to simulate images now from large objects. In this paper, for example what you saw was a set of images of structures that are maybe 500 μm in dimension with fea-

ture sizes less than 1 μm to into tens of micrometers. So the approach has a very nice range of applicability and captures all of the essential physics. It is computationally tractable. So we think it will be very useful.

You state that the paper provides a complete theoretical understanding of image formation in an IR microscope. What was missing from the previous understanding?

Bhargava: Previously, in terms of ray optics, we never explicitly got to include the sample structure in our calculations. So that approach is completely out when you want to look at microscopic objects. In the electromagnetic model, we had never actually modeled the effect of different optics starting from the source to the detector, partly because there would be a lot more detail than is perhaps relevant to what you might need to understand the data or design instruments. And it would take a long time to model each and every component with full electromagnetic theory. In this particular paper, since the model is tractable, we were able to extend it back through all the optics in the system: the interferometer, the image formation optics — the full optics to the detector. In that sense, it's a complete model of light or of how light propagates from the source through the interferometer, through the microscope, through the sample, and then onto the detector. There are no adjustable parameters,

no fitting or empirical parameters. It is a completely analytical expression of how light propagates. And in that sense too it's a complete theoretical model for a Fourier transform infrared (FT-IR) imaging system from the ground up. To my knowledge, this is the first time that's been done.

You comment in the paper that mixing the concepts of resolution and pixel size for correct sampling has led to significant confusion in IR microscopy. Can you explain that?

Bhargava: Yes, that's a great point. On one hand, we have the emergence of the so-called high-definition IR imaging in which we have shown that pixel sizes smaller than the wavelength of light are actually optimal for getting the best image quality that you can get. This is an interesting concept because in the past optical microscopy led us to believe that the wavelength of light and the numerical aperture of the lens are primarily the two things that determine what kind of image quality you might get. In the past, the understanding of this was centered around what we might think of as a spot size that a certain wavelength of light would form at the sample plane. That spot size it traditionally assumed to be roughly equal to the wavelength, However, the spot itself also has some structure to it. It's not a top hat kind of structure. It's got a central maximum and it's got wings in which intensity is distributed and so on. So the first
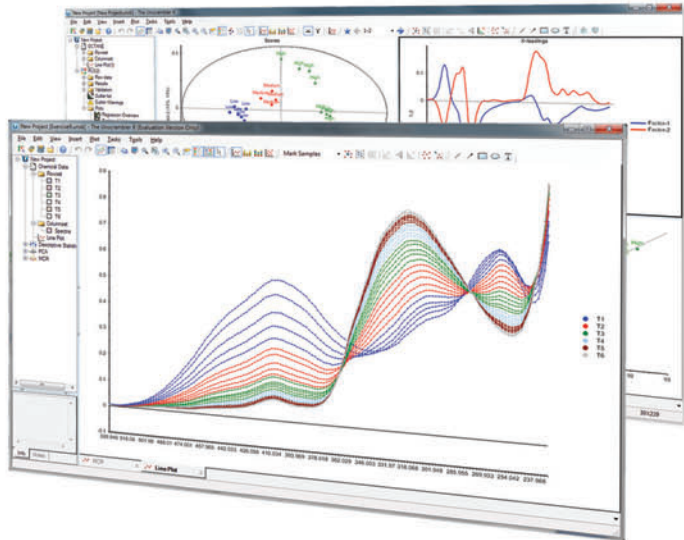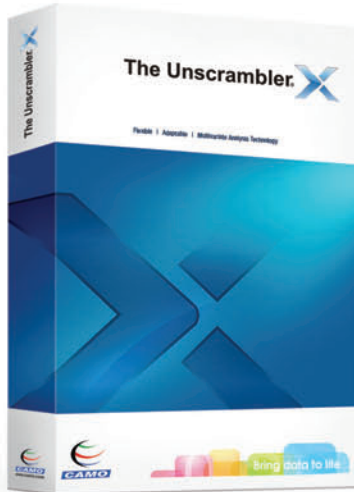
idea is that if you take a high numerical aperture lens, of course you'll get a smaller spot. That is sort of classical physics, there is no confusion there. And if you think that the smallest spot size is what localizes the signal, then to resolve the signal at that spot from another similar spot right next to it is really the resolution criteria that we have known for many hundreds of years. What is known from there is that you must have two features that are separated by a distance such that you can resolve both of them under identical illumination conditions and identical spectral identity. So that part is well established.

Now the question is: If you were to have a pixel size that is exactly at that resolution criterion, are you losing some information? And indeed you are losing information because within that spot, light is not distributed evenly. As said previously, a central maximum and decreasing intensity of light as you move away. So it's got some sort of a curve and to sample a curve within a resolution volume or within a resolution area, you need to sample it more frequently than the size of the curve itself. It's like taking a picture. If you want to capture a picture of an object, then you need to have more than one pixel to sample that object rather than fit it all into one pixel. Similarly, if we want to capture the intensity distribution, we have to have more pixels than simply the total width of the spot. The next question is: How many more pixels do you need — how many pixels are really ideal? That's what this paper tells us from a theoretical perspective — that you need approximately five pixels per resolution element or per wavelength-determined spot size to accurately sample the intensity distribution. It's not to say that within those five pixels you'll be able to resolve features. It's only to say that to sample that spot correctly you need five pixels. Which means that our pixel requirement is actually a little bit higher than we had previously thought. The ideal pixel size to look at the intensity changes in an image is not the size of the wavelength, but

rather maybe a factor 4 or 5 or smaller than that. So in that sense, the resolution concept and the concept of having a certain number of pixels to measure intensity changes in a field of view traditionally have been mixed. This paper separates those two concepts. It says that resolution is where it's determined by classical ideas but the optimal pixel size to sample image features correctly is given in the paper.

How were computer simulations used in the study to analyze the performance of the imaging system?

Bhargava: Computer simulations were used for two reasons. One was fundamentally to validate theoretical model that is based on physics. This is basic science and simulations are the easiest way to predict something from it. The simulations and experiment matched up perfectly in this case. So we can assure ourselves that we have a good model. The second thing that we are using the model for now is to design instruments. So if we want a particular kind of lens or if we have particular wavelengths that we want to measure, then we can use the computer simulations to check if we're indeed getting the performance that we're supposed to get for the samples of interest to us. The third thing, which has not been tackled so far but we're working on it in our lab, is how do we use real-world samples like tissues and polymer samples and use the predictive power of this algorithm, to try to understand what the spectra truly mean in terms of information. This topic has been well explored in the last five years, and the effect of morphology on the data we record is quite profound in some cases. But we don't quite understand fully the science of how different feature sizes, wavelengths, and scattering influence what we can record. These computer simulations would be a great way to systematically understand all these factors. The simulations are very carefully validated now so we can be pretty confident in the results that they give us.

Was the choice of the standard USAF 1951 target as a sample, consisting of

chrome on glass, an important factor in testing the system?

Bhargava: You need some sort of standard sample so we use chrome on glass in this case because there is a very nice, clean difference between the chrome part and the glass part: Glass absorbs pretty much all light at the longer wavelengths and chrome would reflect some of the light back. So it's a very convenient target. Since then we've also developed other USAF targets. There is one that in particular we like: It's a barium fluoride substrate on which we have deposited a lithographically patterned USAF target and there we actually have a polymer that has a spectrum we can measure. In the chrome-on-glass targets, typically your wavelength range is limited and also you don't really have an absorption feature that can be measured. We also don't have a nice absorption spectrum if we wanted to correct for some effects and measure back and correlate. The new target has the same USAF features that are used conventionally in optical microscopy, and the resin is very stable as it is cross-linked, offering a great standard for spectroscopy. The use of this standard target cannot only enable us to correlate theory and experiments but is also useful in comparing the performance of different instruments and for other researchers to use and exchange information using a common basis.

What are some of the challenges you faced when demonstrating the ability to perform high-definition IR imaging in the laboratory by using minimally modified commercial instruments?

Bhargava: The biggest challenge was the low light throughput. When pixels become small, say going from 5 µm to 1 µm, we are only collecting one twenty-fifth of the light that passes through the system. So if you don't change anything else, the signal itself is just one twenty-fifth and the signal-to-noise ratio of the spectrum that you acquire is one twenty-fifth of that obtained previously. So that's the biggest challenge. When you are doing imaging experiments, the signal is low and data are limited in signal-to-noise ratio. The signal-to-noise

ratio is not as high as in conventional spectrometers simply because you are dispersing light over a large area and also because the detectors are not as sophisticated as decades-old single-element detectors. These array detectors used for imaging cannot be particularly sensitive either because of the need to miniaturize electronics. When in high-definition mode, the challenge with low light and with detectors that are not very sensitive becomes magnified. We address that challenge in a number of ways. One of course, is to use better optics, so now we sometimes use refractive optics; other companies have designed better optics for high-definition that can provide more light throughput, longer working distances, and so on. Going from regular definition microscopy to high-definition microscopy, the one overriding challenge is signal-to-noise ratio and other than that everything else is pretty much the same.

In what fields where IR imaging is applied might this approach be a catalyst for improved applications?

Bhargava: I think this approach can be useful in almost every field you can think of. My own personal interests are presently in the biomedical sphere. Here, high definition allows you to see features in tissue and cells that you couldn't see before. It allows a quality of images that just wasn't available before. Now our images look much more like optical microscopy images than like the limited-resolution images that we've seen in the past. It also has very interesting applications for materials science, because sometimes domains are on the order of several micrometers, which was previously spanned by a single pixel and the actual dimensions of the domain could not be seen. Hence, we did not know if we were getting pure spectra. Now, we can start to get a little better visualization than we could before. The same is true for forensics: If there is some small particulate matter, or little bit of evidence that needs to be examined, we can now focus on that little part and see it much more clearly, define it if it's heterogeneous, and look at the heterogeneity with a finer scale. So I think it has implications for all areas of application. Of course, it doesn't provide a solution for every single problem that we might not have been able to solve in the past with IR microscopy. But it is certainly a major step for everybody involved.

What are the next steps in your research with high-definition spectroscopic imaging?

Bhargava: In addition to the challenges presented by having less light throughput, we have many more pixels to scan in high-definition. Again going from 5-µm to 1-µm pixels, there are 25-fold more pixels to scan for the same area to be covered. So speed of data acquisition becomes a major issue. As we continue with high-definition imaging, we are focusing on obtaining faster data acquisition by developing new equipment. Higher speeds can come from hardware improvements in which newer designs, higher throughput spectrometers, newer components like lasers, and more sensitive detectors all play a role. It can also come from software, in which software approaches like those we have used in the past can be used to improve your data quality. That will also drive some applications in our lab. I think the next generation of instruments and applications will come from a combination of hardware, software, and specific driver problems. All three are connected in lots of ways because you need to get a certain quality of data for a specific application typically and you also need hardware of a certain speed if you want to solve the problem in a reasonable period of time. Hardware, software, and new applications that are enabled would be the three major directions for us.

Reference

(1) R. Bhargarva, P.S. Carney, R. Reddy, M. Schulmerich, and M. Walsh, *Appl. Spectrosc.* **67**(1), 93–105 (2013).

This interview has been edited for length and clarity. For more interviews on spectroscopy-related techniques, please visit spectroscopyonline.com/spectroscopy-interviews ∎
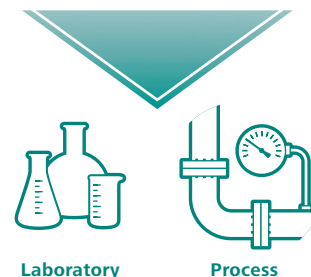
Elemental Analysis of Goji Berries Using Axially and Radially Viewed Inductively Coupled Plasma– Optical Emission Spectrometry

A method for the multielemental determination of metals and nonmetals in goji berries (*Lycium barbarum* L.) by axially and radially viewed inductively coupled plasma-optical emission spectrometry (ICP-OES) is presented. The accuracy of the entire proposed method was confirmed by three certified reference material analyses, and the certified values showed a good agreement at a 95% confidence limit (Student's *t*-test).

Angerson Nogueira Nascimento, Daniel Menezes Silvestre, Flávio de Oliveira Leme, Cassiana Seimi Nomura, and Juliana Naozuka

Goji berries or wolf berries (*Lycium barbarum* L.) have traditionally been used as food and a medicinal plant. The berries grow in China, Tibet, and other parts of Asia. The ripe fruit has been used in Asian countries as a traditional herbal medicine and functional food. The berries are eaten raw, and drunk as a juice, wine, or tea. They can also be processed to form tinctures, powders, and tables (1,2).

The interest in the chemical composition of goji berries has intensified because of an increased awareness of their possible health benefits; they are a rich source of nutrients and phytochemicals, such as organic acids, sugars, phenolic compounds, and minerals (3). Goji berries contain polysaccharides, vitamin C, vitamin B complex, vitamin E, and 18 amino acids (including eight essential amino acids not produced by the human body) (2).

In relation to its elemental chemical composition, studies have shown the presence of 21 elements, including Zn, Fe, Ca, Se, Ge, and P (2). Llorent-Martínez and colleagues (4) determined 26 elements (Ag, Al, As, Ba, Be, Ca, Cd, Co,

Cr, Cu, Fe, Hg, K, Mg, Mn, Mo, Na, Ni, P, Pb, Sb, Se, Sn, Tl, V, and Zn) by inductively coupled plasma–mass spectrometry (ICP-MS) in some exotic superfoods. However, the authors did not detect Ag, As, Be, Cd, Hg, Sb, Se, Sn, Tl, and V in some brands.

Goji berries have been widely used as a popular functional food and are called a "superfruit" or "superfood" because of the large variety of beneficial effects, including reduction of blood glucose levels and serum lipids, anti-aging effects, immune-modulation, anticancer effects, antifatigue effect, and male fertility-facilitatory actions (1,5). Concentrated extracts and infusions show beneficial vision, kidney, and liver functions (1). The recommended dosage of dried berries used as medicine is 5–12 g (6).

Because of the health benefits of goji berries, it is necessary to determine their mineral composition, mainly the essential elements, to deduce the value of this functional food as a mineral source. To accomplish this, the present work reports the results obtained by the proposed method for the simultaneous determination of metals (Al, Ba, Cu, Fe, Mg,

Mn, and Zn) and nonmetals (P and S) in goji berries by using axially and radially viewed inductively coupled plasma–optical emission spectrometry (ICP-OES), following digestion using a diluted oxidant mixture in a closed-vessel microwave oven. The use of a closed-vessel microwave oven and diluted oxidant mixture shows several advantages, such as short heating times (20–40 min), low reagent volume requirements, minimization of residue generation, costs of analysis, and blank values, improving the limits of detection (7).

Experimental

Instrumentation

An iCAP 6300 Duo ICP optical emission spectrometer (Thermo Fisher Scientific) equipped with axially and radially viewed plasma was used throughout. The spectrometer was equipped with a simultaneous charge injection device (CID) detector that measures from 166.25 nm to 847.00 nm. The echelle polychromator was purged with argon. The introduction system was composed of a cyclonic spray chamber and a Meinhard nebulizer. The injector tube diameter of the torch was 2.0 mm. The instrumental parameters were as follows: a power of 1350 W, an auxiliary gas flow rate of 0.2 L/min, a nebulizer gas flow rate of 0.45 L/min, a coolant gas flow rate of 15 L/min, and a pump rate of 25 mL/min. The analytical wavelengths for each element were as follows: Al(I) = 309.200 nm (axial), Ba(I) = 455.404 nm (radial), Cu(II) = 324.700 nm (axial), Fe(I) = 259.948 nm (axial), Mg(I) = 285.213 nm (axial), Mn(I) = 257.618 nm (axial), P(I) = 213.600 nm (axial), S(II) = 180.731 nm (axial), and Zn(I) = 206.200 nm (axial).

An analytical balance (Mettler Toledo) was used to weigh the samples. The samples were dried using a freeze dryer (Thermo Fisher Scientific). After this, the dried goji berries were ground in a knife mill grinder (Grindomix, GM 200, Retsch). The acid sample decomposition was executed in a closed-vessel microwave oven (Speedwave 4, Berghof).

Table I: Figures of merit: linear range, correlation coefficient (R^2), LOD, and LOQ and accuracy evaluation (analysis of CRMs)										
		Al	Ba	Cu	Fe	Mg	Mn	P	S	Zn
Linear range (mg/L)		1–50	1–50	1–50	1–50	1–50	1–50	1–50	1–50	1–50
R^2		0.9998	0.9999	0.9999	0.9998	0.9986	0.9991	0.9998	0.9999	0.9994
LOD (µg/g)		0.8	15	0.64	6	13	7	9	8	13
LOQ (µg/g)		2.7	48	2.13	20	41	22	30	28	45
CRMs Analysis:		Concentration (µg/g) ± Standard Deviation (n = 3)								
SRM 1515	Found	229 ± 60	42 ± 1	4.80 ± 0.14	69 ± 6	0.239 ± 0.012*	51 ± 1	0.146 ± 0.008*	0.15 ± 0.01*	<LOQ
	Certified	286 ± 9	49 ± 2	5.64 ± 0.24	83 ± 5	0.271 ± 0.08*	54 ± 3	0.159 ± 0.011*	0.18*,†	12.5 ± 0.3
Recovery (%)		80	85	85	83	87	94	92	82	ND
SRM 1575a	Found	554 ± 22	<LOQ	2.7 ± 0.2	45 ± 2	0.099 ± 0.0031	503 ± 17	0.102 ± 0.005*	662 ± 20	40 ± 2
	Certified	580 ± 30	6.0 ± 0.2	2.8 ± 0.2	46 ± 2	0.106 ± 0.017*,†	488 ± 12†	0.107 ± 0.08*	545 ± 30	38 ± 2
Recovery (%)		96	ND	94	97	93	103	95	121	105
SRM 3234	Found	ND	ND	13.32 ± 0.20	81.9 ± 1.5	3099 ± 52	35.14 ± 0.49	7055 ± 63	1481 ± 33	51.1 ± 1.0
	Certified	ND	ND	15.34 ± 0.26	80.3 ± 2.7	3487 ± 60	36.78 ± 0.88	8080 ± 210	ND	48.9 ± 1.1
Recovery (%)		ND	ND	87	102	89	96	87	ND	104
* = wt percentage, † = value noncertified, ND = not determined										

Reagents and Samples

All solutions were prepared from analytical reagent-grade chemicals and high-purity deionized water obtained from a Milli-Q water purification system (Millipore). A solution of analytical grade 65% (w/v) HNO_3, distilled in a quartz subboiling still (Marconi) and 30% (w/v) H_2O_2 (Merck) were used for the sample digestion. Analytical-grade Tritisol solutions of 1000 mg/L of Al ($Al(NO_3)_3$), Ba ($BaCl_2$), Cu ($CuCl_2$), Fe ($FeCl_3$), Mg ($MgCl_2$), Mn ($MnCl_2$), P (H_3PO_4), S (H_2SO_4), and Zn ($ZnCl_2$) from Merck were used to prepare the reference analytical solutions for the instrumental calibration. A solution containing 1.0 mg/L of Mg (Merck) was used to evaluate the robustness of the spectrometer (8).

Samples of goji berries (fruit) were purchased from the local market of Sao Paulo, Brazil. Three brands (G1, G2, and G3) and one without a defined brand (G4) were acquired, totaling approximately 250 g of the fruit. The geographic origin (China) was defined for one brand.

The accuracy of the elemental determination method by ICP-OES was evaluated by analyzing three certified reference materials (CRMs) from the National Institute of Standards and Technology (NIST) with a similar sample matrix: apple leaves (SRM 1515), pine needles (SRM 1575a), and soy flour (SRM 3234).

ICP-OES Optimization

The Mg(II) 280.2 nm/Mg(I) 285.2 nm emission line intensity ratio was used to check the robustness of the ICP system (9). The radio frequency power was varied from 750 W to 1350 W and the other instrumental parameters of the spectrometer were held constant.

To check the matrix effects on the sensitivity and selectivity, a scan of the

emission lines was obtained from the standard solution containing 10 mg/L of each analyte and the digested sample. With this experiment, it was possible to choose the best analytical emission line and the signal-to-background ratio (SBR) for all elements. After this, the background correction was manually selected for all the emission lines for quantitative measurements.

The limits of detection (LOD) were calculated using the background equivalent concentration (BEC) and SBR, according to the International Union of Pure and Applied Chemistry (IUPAC) recommendations (IUPAC, 1978):

$$BEC = C_{rs}/SBR, SBR = I_{rs} - I_{blank}/I_{blank},$$
$$LOD = 3 \times BEC \times RSD/100 \qquad [1]$$

where C_{rs} is the concentration of the multielemental reference solution (10 mg/L), I_{rs} and I_{blank} are the emission intensities for the multielemental reference (10 mg/L) and blank solutions, and RSD is the relative standard deviation for 10 consecutive measurements of a blank solution. The limits of quantification (LOQ) were calculated as 10 × LOD (8).

Sample Preparation
Approximately 30.0 g of each goji berry sample was dried in the freeze dryer for 48 h. The dried samples were ground in a knife mill grinder, applying two cycles of 5000 rpm for 30 s. The acid decomposition was performed in a closed-vessel microwave oven using 0.2 g of the sample or CRMs and the diluted oxidant mixture, containing 2.0 mL of nitric acid (65%, v/v), 1.0 mL of hydrogen peroxide (30% v/v), and 3.0 mL of deionized water. The heating program was executed in three steps: step 1 (temperature: 140 °C, ramp: 5 min, and hold 1 min), step 2 (temperature: 140 °C, ramp: 4 min, and hold 5 min) and step 3 (temperature: 200 °C, ramp: 4 min, and hold 10 min), using

Table II: Elemental concentration in goji berries obtained by ICP-OES			
Concentration (µg/g) ± Standard Deviation (*n* = 3)			
	G1	**G2**	**G3**	**G4**
Al	49 ± 6	42 ± 6	52 ± 5	39 ± 2
Ba	<LOQ	<LOQ	<LOQ	<LOQ
Cu	6.9 ± 0.2	6.5 ± 0.1	5.9 ± 0.3	5.2 ± 0.1
Fe	62 ± 6	56 ± 5	69 ± 5	58 ± 3
Mg	1061 ± 66	686 ± 42	646 ± 19	834 ± 44
Mn	<LOQ	<LOQ	<LOQ	<LOQ
P	2060 ± 142	1637 ± 89	1450 ± 54	1892 ± 62
S	956 ± 6	672 ± 7	566 ± 21	621 ± 13
Zn	<LOQ	<LOQ	<LOQ	<LOQ

725 W of power and a maximum pressure of 50 bar. The final volume was diluted up to 10.0 mL with deionized water. The digestion procedure was done in triplicate for each sample.

Results and Discussion

Analytical Performance of ICP

The term *robustness* was proposed to represent the efficiency of the energy transfer and response of the plasma to a change in the atomization and excitation conditions, and the chemical composition of the aspirated solution. When the plasma operation is close to the local thermodynamic equilibrium, the Mg(II)/Mg(I) ratio is higher than 8. This value indicates an effective energy transfer from the plasma to the analytes flowing through the central channel (9). A good response was observed using the standard nebulizer gas flow rate of 0.45 L/min.

Maintaining the same outer gas, the best raw intensity to background ratio was obtained when 1350 W was applied. Under these conditions, the Mg(II)/Mg(I) ratios were 12.4 and 10.3 for axially and radial viewed, respectively.

Figures of Merit

Characteristic parameters of the analytical calibration curve, such as linear range, correlation coefficient (R^2), limits of detection (LOD), and limits of quantification (LOQ), are presented in Table I. The LOD and LOQ are obtained in micrograms per gram by considering the sample mass of 200 mg and a final volume of 10 mL. The average RSD (%) for repeatability of the calibration solution measurements ($n = 5$) ranged from 0.25 (for Ba and Zn) to 0.39 (for P). The average RSD values for the repeatability of digested sample measurements ($n = 3$) varied from 3.7% (for S) to 14% (for Ba), providing evidence of a good level of precision. The worst result was observed for Zn (RSD = 27% only for the G3 sample).

The quality of the results obtained by using the entire analytical procedure were checked by analyzing three CRMs, which were subjected to the same experimental steps adopted for the samples. The comparison between the experimental and certified values for all analytes is presented in Table I. The results obtained showed that the method is selective and accurate. They are in good agreement considering a Student's *t*-test at a 95% confidence limit.

It is important to point out that the CRM analysis allowed us to verify the sample digestion efficiency in a closed-vessel microwave oven, with the diluted oxidant mixture and an absence of chemical and spectral interferences during elemental determination by ICP-OES. The oxidant mixture of $HNO_3 + H_2O_2$ provides a high oxidizing power, aided by the presence of water. Water is a highly dipolar molecule, and thus it is suitable for an efficient interaction with microwave radiation. Hence, the use of water promotes an increase in the pressure and temperature inside the closed vessels during sample digestion (8).

Elemental Composition of the Samples

The element concentrations using the robust conditions previously established are shown in Table II. The standard deviations (SD) are related to the expanded error associated with the instrument measurements ($n = 3$) and the three analyses of each sample. As expected, Mg, P, and S can be considered the macroelements in these samples. It is important to highlight that essential and nonessential element concentrations are dependent on the soil characteristics, the physiology of the plant, the water source composition, and fertilizers, insecticides, pesticides, and fungicides used at the plantations. Plants can absorb, carry, and accumulate chemical elements. Each species has its own requirements and differing levels of tolerance when absorbing and accumulating an element. The movement of the inorganic constituent is selectively controlled by the plant, with some being easily absorbed and others impeded to different degrees (7).

Studies involving the chemical composition of superfoods are important from nutritional and toxicological points of view. The amount of an essential nutrient considered adequate for human requirements is termed the *dietary reference intake* (DRI). The Food and Drug Administration (FDA) regulations require nutrition labeling for most foods. Reference daily intakes (RDIs) for some essential human nutrition elements and daily reference values (DRVs) have been established, namely Cu (2 mg), Fe (18 mg), Mg (400 mg), Mn (2 mg), P (1000 mg), and Zn (15 mg) (10). Considering the concentration of the elements on the different goji berry samples (Table II) and the recommended manufacturer dosages of 10 g and 30 g (4), the masses of these elements ingested were 52–207 µg (Cu), 0.56–2.1 mg (Fe), 6.5–32 mg for Mg, and 15–62 mg for P. Considering a goji berry consumption of 30 g, the contribution percentages to DRVs were 11%, 12%, 8%, and 6% for Cu, Fe, Mg, and P, respectively.

In general, the elemental concentrations in all samples decreased in the following order: P > Mg > S > Fe > Al > Cu. For all the study samples, the Ba, Mn, and Zn concentrations were below the LOQ. The difference in the elemental concentration between the samples can be the result of variations in the geographic origin and cultivation conditions. There are approximately 70 species of *Lycium* growing in temperate to subtropical parts of North America, South America, southern Africa, Eurasia, and Australia (1).

Analytical methods for essential element determinations in the goji berry are still limited. It is imperative to acquire more information about the chemical composition and conduct studies on the chemical speciation and bioavailability of this functional food. At the same time, toxic element concentrations should also be determined. Llorent-Martínez and colleagues (4) found low concentrations of Cd, Pb, and Sn that did not represent a risk to human health. Additionally, there is no known toxicity reported on the goji berry in the scientific literature or in traditional Asian herbal medicine textbooks (1).

Conclusions

A simple, robust, and reliable analytical method for the simultaneous

determination of macro- and microelements in goji berries by axially and radially viewed ICP-OES was established. By analyzing three CRMs, it was observed that the effectiveness of a closed-vessel microwave oven in combination with the diluted oxidant mixture (2.0 mL HNO_3 + 1.0 mL H_2O_2 + 3.0 mL H_2O) to digest the high organic content of the samples analyzed in this work and absence of chemical and spectral interferences in the elemental determination by ICP-OES. The results presented in this article enhance the knowledge of the elemental composition of goji berries, a superfood, widely consumed for their functional properties. Additionally, this work will help aggregate information in the toxicological and nutritional fields.

Acknowledgments

References

(1) H. Amagase and N.R. Farnsworth, *Food Res. Int.* **44,** 1702–1217 (2011).

(2) P.G. Pai, U. Habeeba, K. Ramya, M.S. Pradeepthi, and Y. Belagali, *Int. J. Pharm. Sci. Res.* **5,** 1411–1415 (2014).

(3) M. Mikulic-Petkovsek, V. Schmitzer, A. Slatnar, F. Stampar, and R. Veberic, *J. Food Sci.* **77,** C1064–C1070 (2012).

(4) E.J. Llorent-Martínez, M.L. Fernández-de Córdova, P. Ortega-Barrales, and A. Ruiz-Medina, *Microchem. J.* **110,** 444–451 (2013).

(5) Q. Luo, Y. Cai, J. Yan, M. Sun, and H. Corke, *Life Science* **76,** 137–149 (2004).

(6) O. Potterat, *Planta Med.* **76,** 7–19 (2010).

(7) J. Naozuka, E.C. Vieira, A.N. Nogueira, and P.V. Oliveira, *Food Chem.* **124,** 1667–1672 (2011).

(8) G.C.L. Araújo, M.H. Gonzalez, A.G. Ferreira, A.R.A. Nogueira, and J.A. Nóbrega, *Spectrochim. Acta* **57B,** 2121–2132 (2002).

(9) J.M. Mermet and E. Poussel, *Appl. Spectrosc.* **49,** 12–18 (1995).

(10) S.P. Dolan and S.G. Capar, *J. Food Compos. Anal.* **15,** 593–615 (2002).

Angerson Nogueira Nascimento and Juliana Naozuka are with the Universidade Federal de São Paulo in São Paulo, Brazil. **Daniel Menezes Silvestre Flávio de Oliveira Leme, and Cassiana Seimi Nomura** are with the Instituto de Química at the Universidade de São Paulo in São Paulo, Brazil. Direct correspondence to: jnaozuka@gmail.com ∎

For more information on this topic, please visit our homepage at: www.spectroscopyonline.com

Quantifying Proteins by Mass Spectrometry

The quantification of proteins in a complex biological sample is an important and challenging task. Mass spectrometry (MS) is increasingly used for this purpose, not only to give a global survey of the components and their amounts, but also to precisely and accurately quantify specific target proteins. Here, we review the essential elements of MS approaches to protein quantification and critically compare the available options.

Mark W. Duncan, Alfred L. Yergey, and P. Jane Gale

Proteins are the most abundant macromolecules in biological systems. Together with their smaller relatives, peptides, they are polymers comprising amino-acid building blocks joined through amide bonds. In contrast to the repeating units of other biopolymers (for example, polysaccharides and polynucleotides), the constituent amino acids are diverse in their chemical and physical properties. Consequently, the polymers derived from them are also a complex, chemically and physically diverse ensemble.

This structural diversity lends itself to extensive functional diversity. Proteins serve as antibodies, enzymes, messengers, structural components, and transport or storage molecules. For that reason, the majority of drug targets are proteins. Significantly, the genetic machinery of the cell is tasked with synthesizing proteins. Accordingly, one might argue that much of each cell, and therefore any organism in toto — its structure, function, reproduction, repair, and regulation — relies on proteins. Understanding biology — function or dysfunction, health or disease — is therefore about defining and understanding proteins.

Protein identification and quantification are thereby the two central objectives of many biological and biomedical studies. Historically, these tasks were performed on purified proteins that were exhaustively sequenced (such as Edman) or quantified by the immuno-based western blot or enzyme-linked immunosorbent assays (ELISAs). Today, however, because of advances in mass spectrometry (MS) and the development of a set of global, protein-analysis tools that some call the "proteomics toolbox," improved analytical strategies have evolved, and the objectives of researchers have changed. Typically, investigators now aim to study biological entities at the "systems" level; that is, they seek to resolve and identify a multitude of proteins simultaneously in a single sample and to quantify each in relative or absolute terms. (See definitions in Table I.)

Quantification is an important component of most studies. Defining differences or changes in protein abundances (or, more appropriately, the abundance of specific protein species including isoforms and post-translational variants) between two or more groups or states (such as control and test) is often at the heart of understanding function and regulation.

As the proteomics toolbox evolves, new approaches to protein quantification by MS are continually reported. These methods can be categorized into several major classes, all of which share features and performance characteristics. Furthermore, though some additional considerations are specific to protein quantification, it is also important to state that the process of quantification remains essentially the same, regardless of the nature of the analyte (that is, small molecules versus biopolymers). Consequently, the principles and practices that have guided the development and evaluation of quantitative methods (for example, replicate measurements to characterize the variance of a method) are no less applicable in this setting.

Non-MS Approaches to Protein Quantification

This column installment focuses on MS methods for protein quantification because of their growing importance. Yet it is important to acknowledge the existence of other strategies and that, moreover, in certain settings those alternatives may be the methods of choice. For example, the mainstay for targeted protein quantification for almost 50 years has been the western blot immunoassay, in which antibodies are used to detect proteins transferred from polyacrylamide gels to nitrocellulose or polyvinylidene fluoride membranes. Refinements of the basic protocols yield detection limits in the attomolar range (1). Evolution of the principles underlying the western blot led to the development of the radioimmunoassay (RIA) and ELISA (2,3). In a clinical setting, specific proteins are commonly quantified by ELISA. Similarly, for several decades, quantification of multiple

More coHAIRence

When you can't afford a bad laser day

Cobolt
www.cobolt.se

ENESTEDT.SE

Table I: Some essential definitions

Term	Definition
Relative quantification	Relative quantification strategies compare the levels of individual proteins in a sample to those in another sample. Results are typically expressed as a relative fold change, or percent change, of protein abundance.
Absolute quantification	Absolute quantification is the determination of the amount, in units of mass or concentration, of a protein in a sample. For example, protein X expressed in units of nanograms per milliliter of plasma.
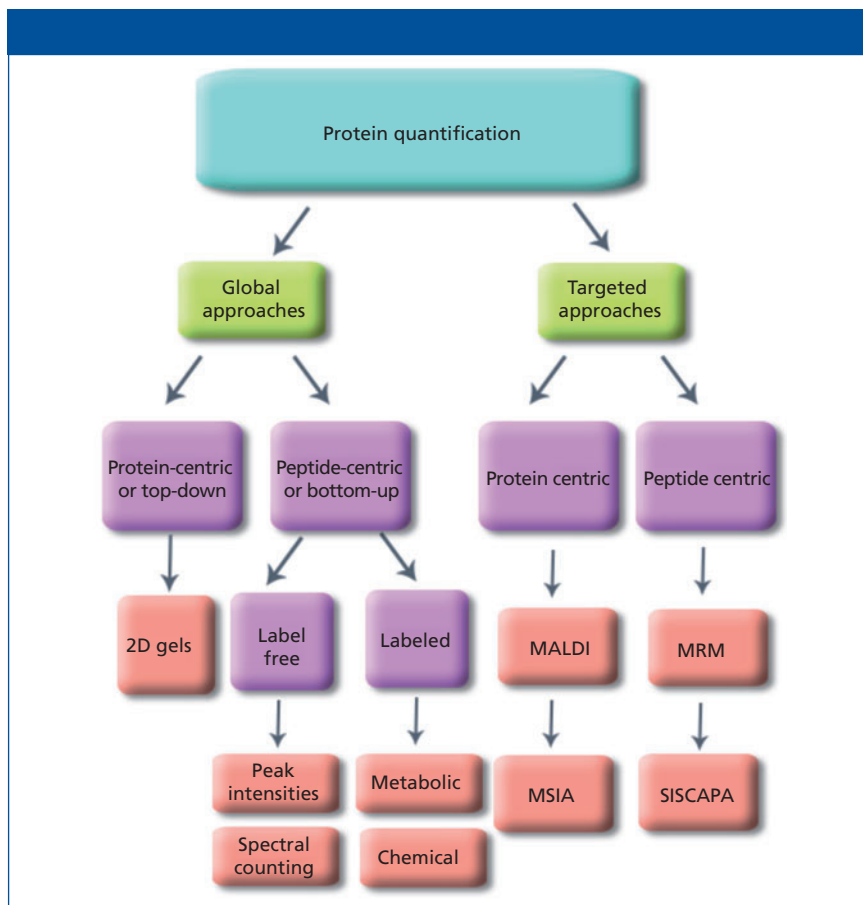
Figure 1: Diagrammatic representation of the common strategies for protein quantification and the relationships between them.

protein components in complex biological samples has relied on two-dimensional (2D) gel electrophoresis (discussed in some detail later). Additionally, a growing array of multiplexed, selective capture methods, including aptamer and antibody arrays, are increasingly used for protein quantification. Numerous reviews discuss these and related strategies (4–9).

MS Approaches to Protein Quantification

An Overview of the Approaches

We categorize protein quantification by MS into several groups. These are out-lined below, represented in Figure 1, and discussed in more detail in the sections that follow.

Global, System-Wide (Multicomponent) Strategies

Here, hundreds or thousands of proteins are compared in two or more samples and quantification is typically relative. Nevertheless, with modification to the basic method, absolute quantification is sometimes possible.

Protein-Centric or Top-Down Strategies

These approaches involve resolution of a complex mixture of proteins (for example, by 2D gel electrophoresis) and quantification in their intact form. The approach often involves differential radio- or chemical-labeling of proteins in distinct samples (such as, difference gel electrophoresis [DIGE]). After tagging, the samples are combined, the proteins are resolved in two dimensions, and the relative amounts of the tagged proteins are measured. Protein spots are excised from the gel, digested, and identified by MS by means of peptide mass maps (that is, peptide masses), peptide sequences (that is, tandem mass spectrometry [MS-MS]), or a combination of both techniques.

Peptide-Centric, Bottom-Up, or Shotgun Strategies

Here, a complex mixture of proteins, an extracted proteome, is digested to peptides. The peptides, which serve as surrogates of the original intact proteins, are then separated, quantified, and identified. These strategies are further subdivided into label-free strategies and labeled strategies, depending on whether a label is incorporated:

Label-Free Strategies:
- Isolate proteins in a sample → proteolysis → separate peptides → sequence peptides → identify protein → repeat procedure for additional samples. We then compare either the number of peptides recovered for each protein (that is, spectral counts) or relative abundances of specific peptide ions (that is, peptide peak intensities by liquid chromatography–mass spectrometry [LC–MS]) to quantify proteins.

Labeled Strategies:
- This involves differential metabolic labeling with stable isotopes of proteins in two or more samples → combine samples → isolate total proteins → proteolysis → separate peptides → quantify differentially labeled peptides → sequence peptides and identify proteins (for example, stable isotope labeling by amino acids in cell culture [SILAC]).
- Differential chemical labeling with stable isotopes of proteins in two or more samples → combine samples → isolate total proteins → proteolysis → separate peptides → quantify

differentially labeled peptides → sequence peptides and identify proteins (for example, isobaric tags for relative and absolute quantitation [iTRAC]). (Note the similarities of this approach to DIGE. The primary difference is that separation and quantification are performed on surrogate peptides, not intact proteins.)

Targeted (Single-Component or Several-Component) Quantification Strategies

In these approaches one or a few components are selectively isolated from a sample and quantified in relative or absolute terms. Approaches fall into two categories, top-down and bottom-up.

Top-Down Approach

Direct quantification by matrix-assisted laser desorption-ionization (MALDI) or protein isolation–concentration by an approach such as mass spectrometric immunoassay (MSIA, Thermo Fisher Scientific): Selective isolation of one or more proteins → determine protein abundances based on ion current. Protein identification or selectivity is derived from antibody and mass of target protein; amount is based on ratio of peak heights/areas for analyte and an internal standard. Absolute concentrations are determined referring to a calibration curve containing a fixed amount of internal standard (IS) and varying amounts of the intact target protein.

Bottom-Up Approach

Multiple-reaction monitoring (MRM) methods including stable isotope standard capture with anti-peptide antibodies (SIS-CAPA). Approaches selectively isolate target protein or proteins → digest proteins → quantify one or several peptides according to parent-ion (MS) or product-ion chromatograms (MS-MS).

General Considerations in Quantitative Proteomics by MS

An abundance of reviews discuss protein quantification by mass spectrometry, but most focus on instrumental considerations (10–13). Furthermore, most authors have almost exclusively focused on electrospray ionization (ESI)-based approaches and have neglected the findings of precise and sensitive intact-protein quantification by MALDI-based methods. Our focus is on the overarching steps in system-wide protein quantification.

Sources of Inaccuracy and Imprecision

Multiple sample-manipulation steps are common before instrumental analysis (for example, protein precipitation or isolation, fractionation, selective depletion and enrichment, proteolysis, and tagging and labeling reactions). Each step is a source of preanalytical sample variability that can compromise both precision and accuracy. For example, high-abundance proteins like albumin are sometimes removed from plasma samples by means of immunodepletion before analysis. However, that removal process introduces a risk of codepleting other components of interest because of nonspecific binding to both the antibodies used and to the albumin itself (by other sample components). Similarly, other steps such as protein precipitation and enzymatic digestion can introduce significant imprecision and inaccuracy because proteins are not recovered or digested quantitatively. Irreproducibility

Make the SMART move to PDF-4+

ICDD databases are the only crystallographic databases in the world with quality marks and quality review processes that are ISO certified.

S Standardized data

M More coverage

A All data sets are evaluated for quality

R Reviewed, edited and corrected prior to publication

T Targeted for material identification and characterization

PDF-4+ 2014 features over 354,000 entries including 239,000+ entries with atomic coordinates.

ICDD International Centre for Diffraction Data

ISO 9001:2008 QUALITY ASSURED COMPANY CERT.NR. 11405/1

www.icdd.com | marketing@icdd.com

in other sample-handling steps, including chemical labeling, together with instrument perturbations (such as pressure and temperature fluctuations and tuning); the laboratory environment (for example, temperature and humidity); reagent variability; the presence of coeluted species or their levels; and analyte concentration can contribute to imprecision by altering the ionization process and thereby the measured signal intensity. Intensity comparisons are therefore compromised at a fundamental level. Studies that compare results across different analytical runs are most susceptible to these factors. Minimizing or carefully controlling key variables is critical. Yet even so, given the number of steps in the analysis and the number of species being measured, many potential sources of imprecision remain.

Validation of Proteomic Methods

It is important to remain mindful that the primary aim of any quantitative proteomics study is to provide timely, accurate, and reliable data that are fit for an intended purpose. Nevertheless, depending on the specific approach and the rigor with which the analysis is performed, the quality of the data will be variable and undefined. Quantifying thousands of components in a sample is a formidable challenge, to say the least. Defining specificity, linearity, accuracy, precision, range, detection limit, upper and lower limits of quantification, and robustness — all central considerations in the validation of a conventional quantitative analysis — is, given the scope of the task, empirically impossible for every protein species. Similarly, recovery and stability studies are not possible on each of the components. Consequently, in global proteomic studies, validation of the assay is typically perfunctory, and the resultant data are of uncertain and ill-defined reliability.

Although conventional validation is not practical, measures of precision and accuracy remain essential so that experimental findings can be put into context. Therefore, we must be confident that the measured differences are real and not merely an artifact of the method itself.

A method's assessed precision for a subset of analytes measured, at various concentrations, in one or more test samples and the derived data can be used to determine the method's suitability. These data can also help validate subsequent findings derived from the method (14). Similarly, technical replicates (that is, repeat analyses of each of the samples in the study) provide additional support that a change is real, not an artifact of the analytical method itself. In the same vein, the issue of specificity must also be considered.

Accurate quantification cannot be assumed on the basis of one — or even a few — peptides simply because a single peptide defines only a single segment of any protein, and modifications elsewhere in the molecule are missed (14,15). Quantification based on a peptide common to multiple, related forms will always lead to an overestimate of the amount of any single variant whereas quantification based on a unique peptide fails to "recognize" and quantify closely related variants of that protein, even if they are significantly more abundant. Precise and accurate quantification of a specific protein variant is therefore achievable only when the targeted peptide or peptides are derived from

SPIE. PHOTONICS WEST

²⁰15

PHOTONICS WEST.

THE PREMIER EVENT FOR THE PHOTONICS AND LASER INDUSTRIES

REGISTER TODAY

WWW.SPIE.ORG/2015PW

BiOS—Biomedical Optics
Translational Research
LASE—Lasers and Sources
OPTO—Optoelectronic Devices
Green Photonics
3D Printing
Industry Panels and Keynotes

The Moscone Center
San Francisco, California, USA

Conferences & Courses
7–12 February 2015

Photonics West Exhibition
10–12 February 2015

BiOS EXPO
7–8 February 2015

a single precursor protein or, in the case of protein-centric methods, in instances in which we can resolve and quantify the specific (intact) protein species without interferences.

The situation, however, is not as bad as it might seem at first. Because a common objective in proteomics is to compare groups — for example, disease versus control or control versus test — absolute levels are not (necessarily) important. Defining percent change (or difference) is the overarching objective. Therefore, it is possible to take advantage of differential (isotopic) tags and the exquisite selectivity of mass detection to compare two (or more) samples worked up and assessed in the same experimental run under identical conditions. For example, in a typical experiment all proteins in a sample (such as control) are labeled with a chemical tag; separately, all of the proteins in a second sample (such as disease) are labeled with an isotopic variant of the same tag. The samples are then mixed and treated as one. Thereafter, each tagged protein and its isotopic variant behave in an identical manner during sample handling. Yet because of their difference in mass, they can be specifically detected and quantified by MS. While this detection and quantification strategy markedly reduces variance in one sense, such an approach is limited to "A versus B" comparisons. Numerous modifications of the basic strategy have been developed and will be discussed in more detail later in this installment.

Global or Proteome-Wide Protein-Centric Quantitative Tools

2D Gel-Based Methods

Using 2D gel-based methods is the most frequently adopted top-down strategy, and it is based on quantitative analyses of intact proteins resolved via 2D gel electrophoresis. Typically, the first step is protein separation by isoelectric focusing (IEF; first dimension [1D]) and then orthogonal separation of the proteins distributed on the 1D strip by sodium dodecyl sulfate–polyacrylamide gel electrophoresis (SDS-PAGE; second dimension). Protein spots (that is, discrete species) are visualized by dyes, fluorophores, or radioactive labels tagged. (These can be visible or fluorescent post-electrophoretic dyes, or fluorophores or radioactive labels that are tagged to proteins before resolution. Examples include silver stain, Pro-Q Diamond, 2,4-dinitrophenylhydrazine, or Coommassie blue.) The quantity of each protein is assessed by measuring the spot's density using a customized software package. Two-dimensional gels provide excellent sensitivity, precision, and linearity over a wide dynamic range. Nevertheless, subsequent identification of proteins requires resecting, by hand or robot, the individual spots from the gel followed by MS (that is, a peptide mass map with or without additional MS-MS sequence information).

To minimize the influence of gel-to-gel variations, and to reduce the total number of gels required, variants of this general strategy involving differential labeling (or tagging) of the proteins in two or more samples have been developed (for example, with fluorophores or radioactivity labels). The objective of these approaches is to retain the physical properties of the proteins so that their mobility in each of the two dimen-

sions of separation remains unchanged. Therefore, both can be run as a mixture on one gel, and each can be independently quantified, because of the tag.

The most common manifestation of this approach is DIGE (16). Here, three (or more) different protein-containing samples can be labeled with size-matched, charge-matched, spectrally resolvable fluorescent dyes (for example, Cy3, Cy5, and Cy2) before 2D gel electrophoresis. In this way, the number of gels to be resolved is reduced, precision is increased, and the time and cost of the comparison is also reduced. For example, running two samples on a single gel significantly increases reproducibility. Nevertheless, because three distinct "tags" are available, comparisons can also be made between multiple samples run across multiple gels by using a pooled internal standard (17). Composed of a mixture of all of the samples constituting the study, this standard is tagged and run on each gel. The pooled sample acts as an internal standard for every protein spot on each of the gels. As such, it is used to normalize all

spots and to optimize inter-gel precision. Typically, reciprocal labeling (a dye-swap experiment) is performed to ensure the observed changes are not associated with dye-dependent interactions. Commercial software is used to detect differences and assign statistical confidence to them.

Critical Evaluation

With high precision, 2D gel electrophoresis and its variant, DIGE, allow relative abundance comparisons that detect modest changes of one to several thousand proteins in multiple samples. Provided they can be resolved, variant forms of the same protein (that is, protein variants or proteoforms) can also be independently quantified. Because each separation is visually represented, only proteins that differ in abundance need be resected from the gel and identified. Two-dimensional gel electrophoresis and DIGE have been successfully adopted by many investigators. Both methods have been thoroughly reviewed and have stood the test of time (18,19). However, the approach is cumbersome,

labor-intensive, and difficult to fully automate. These limitations, especially the last, have dampened the enthusiasm of many to adopt 2D gel electrophoresis (and DIGE). While it is frequently suggested that the resolution of a 2D gel is limited, it is important to stress that no other approach rivals 2D gel electrophoresis for practical, intact protein separation. Comigration of multiple proteins to the same location on the gel is also often cited as a problem, but it is rarely an issue (20). Similarly, although large (>150 kDa) or small (<5 kDa) proteins are difficult to separate on gels, this difficulty is not a significant limitation because work-arounds are available, at least for peptides. DIGE is subject to variations in the extent of labels incorporated into the proteins, a potential source of variance in the measurements. Identifying proteins is sometimes problematic, especially with DIGE. Alignment problems can occur because identification requires running a separate (preparative) gel and then matching it to images for the set of analytical gels.

Other Top-Down Strategies

In this review, we forego discussion of instrument-intensive, top-down approaches simply because they are not yet practical for routine use. As alternatives to 2D gel, top-down proteomic approaches are, however, being developed by several groups. These alternatives involve introducing intact proteins into a mass spectrometer and fragmenting them directly. By working with the intact protein, complete sequence coverage is possible, and post-translational modifications (PTMs) are preserved. Until recently, however, top-down proteomic strategies were restricted to the analysis of purified proteins or simple mixtures. Over the last few years the approach has been extended to complex mixtures of proteins (21), but quantification remains a challenge nonetheless.

Global or Proteome-Wide Peptide-Centric Approaches

General Comments

Peptide-centric (bottom-up or shotgun) quantitative strategies are dominant because of their purported ability to quantify multiple components simultaneously in an automated or semiautomated manner. These strategies involve a common step: that is, site-specific cleavage of a mixture of isolated proteins (a proteome) to generate a substantially more complex mixture of peptides. Typically, peptide-centric applications utilize trypsin and quantify based on tryptic peptides. The selective cleavage of proteins to peptides is undertaken for these reasons: Peptides can be separated by LC better than proteins; most proteins generate one or more soluble peptides even if the antecedent protein is poorly soluble; peptides fragment better in a tandem mass spectrometer, giving spectra that can be sequenced; and peptides can be detected at much lower levels than their protein precursors. The peptides are then fractionated by LC and analyzed by MS-MS (14).

It is important to acknowledge, however, that all peptide-centric approaches to quantification are based on the assumption that when a protein is cleaved by a specific reagent, the reaction will go to completion, or at the very least, that the cleavage will be reproducible and predictable. Further, it is assumed that the target peptide or peptides are sufficient to define

and selectively quantify the antecedent protein (that is, the target peptide is solely derived from a single antecedent protein). In practice, however, a target peptide or peptides may be degenerate and shared by multiple proteins. Through digestion, connectivity between the peptides and their antecedent protein is lost, a phenomenon referred to as the *protein inference problem* (22). In fact, multiple variants of a protein (variant protein species or proteoforms) are common, and unless peptides incorporating the specific, modified residue or residues (for example, the oxidized, reduced, nitrated, phosphorylated, glycosylated, or differentially "altered" amino acid) are targeted, quantification will be inaccurate. As a specific example, a single-point amino acid mutation may exist in a target protein, but if quantification is based on any tryptic peptide other than the one incorporating the modification, the variant will not be detected. Similarly, other variants of the precursor protein including truncated or alternatively spliced forms are often misidentified (15). On the other hand, if the focus is on identifying specific modifications, and the correct peptide is targeted, the peptide-centric approach offers advantages. The influence of a modification on mass is more evident at the level of the peptides than it is at the protein level because the percent change in mass is greater.

Relative quantification by peptide-centric methods can involve the separate analysis of multiple samples by MS and their subsequent comparison (for example, label-free methods). Alternatively, tags (such as isotopic tags or stable isotopes) can be incorporated into proteins or their proteolytic peptides. These cause a shift in mass of the labeled protein or peptides in the mass spectrum. Differentially labeled samples can be combined and analyzed together, determining differences in the peak intensities of the isotope pairs. These intensity differences correlate with differences in the abundance of their antecedent proteins.

With these overarching issues in mind, the approach can be implemented in many, disparate ways. This review does not aim to be an encyclopedia of all available methods. Instead, it is a description of the basic divergent strategies and their strengths and weaknesses.

Label-Free Approaches

Label-free quantification is fast, cost-effective, and easy to implement. It is frequently used when stable isotope incorporation is impractical or cost-prohibitive. In these approaches, samples are analyzed separately and results from multiple runs are compared. The two main, label-free approaches each rely on proteolytic digestion of a sample followed by analysis by LC–MS or LC–MS-MS. Both strategies are used to make comparisons between two or more samples and to determine relative change in protein abundance (with the caveats noted above).

Spectral Counting

This is a practical, semiquantitative measure of protein abundance in proteomic studies. Relative quantification by spectral counting compares the number of identified spectra associated with the same protein between different samples — that is, the total number of tandem mass spectra that match peptides to a particular protein as a measure of protein abundance within a complex mixture. The approach is based on the finding that increasing protein abundance results in an increase in protein-sequence coverage. Therefore, abundant proteins produce more MS-MS spectra than less-abundant proteins, and their antecedent peptides are sampled more often in fragment-ion scans than those derived from low-abundance proteins. However, important caveats are associated with this approach. Low-mass proteins (that is, those generating fewer fragments on proteolysis) are problematic; the dynamic range of the approach is limited; precision is poor and, consequently, small changes in protein abundances are difficult to determine. Several modifications of spectral counting, including the normalized spectral abundance factor (NSAF) approach (23), have also been reported. NSAF corrects for the fact that larger proteins yield more peptides on digestion than shorter proteins and also accounts for sample-to-sample variations associated with replicate analysis. A modified spectral counting strategy, absolute protein expression (APEX) profiling, has been used to measure the absolute protein concentration per cell after the application of several correc-

tion factors (24). Further refinements have also been made and the approach was recently reviewed (25).

Quantification Based on Peptide Peak Intensities as Determined by LC–MS

This approach to quantification is based on the observation that for a specific peptide separated and detected by LC–MS, the measured ion current increases with increasing concentration. Typically, ion chromatograms for each peptide of interest are extracted from an LC–MS run, and their peak areas are integrated over time. Peak areas for the same ion are then compared between different samples, to give relative quantification; absolute amounts can also be calculated by reference to a calibration curve. Most often, ion currents derived from the intact, protonated, peptide ions are monitored, but product ions generated by MS-MS can also be used for quantification. (Product-ion detection increases selectivity, but at the expense of sensitivity.) The approach and computational strategies to manage the data have been reviewed (26).

While the relationship between the actual amount of protein and generated ion current holds true for standard samples of limited complexity, in practice, the analysis of digests of complex biological samples is far more problematic. For example, variations in temperature, pressure, sample preparation, injection volume, retention time, and the presence of coeluted species can significantly compromise precision. (Studies often extend over weeks — or even months — and changes in column, mobile phase, instrument condition, and calibration begin to manifest themselves.)

Critical Evaluation of Label-Free Approaches

Label-free approaches are inexpensive and simple to implement, but the old aphorism, "You get what you pay for" may apply. They allow "semiquantitative" comparisons between samples, but precision and reliability is low, in large part because without an internal standard the measured ion current is susceptible to many factors when it is measured in many separate runs. In a recent study by The Association of Bio-

molecular Resource Facilities (ABRF), data generated from digests of parallel lanes of gel-separated proteins were supplied to several groups. The task was to "identify" the proteins in the sample and determine which were elevated or reduced in intensity relative to the adjacent lane. Not surprisingly, participants failed to agree, and there was no evidence that either approach — spectral counting or intensity-based quantification — could reliably address this question (27).

Labeled Approaches to Global Protein Quantification
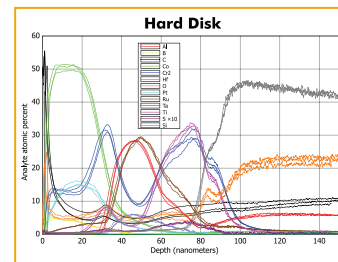
General Comments

These approaches uniquely tag the proteins in two or more samples with a stable-isotope tag. The tagging can be done metabolically (that is, by adding enriched amino acids into cell culture medium) or chemically (that is, by covalently binding a labeled moiety to the proteins). The samples are then combined and analyzed in a single run. Precision is markedly improved

because two or more samples are compared within one run, but at the expense of the time, cost, and complexity of the overall analysis. The earlier in the analytical process the label is incorporated into the proteins, the better, but its (global) incorporation is far from straightforward.

Metabolic Labeling

In this approach to relative quantification, the proteins in two or more samples are labeled with isotopically distinct forms of amino acids by growing cells in enriched culture medium (for example, SILAC). The first report of this approach was by Ong and colleagues in 2002 (28). Typically, two populations of cells are grown in separate cultures, one in standard medium and the other in medium containing stable-isotope-labeled amino acids. After the samples are combined, the mass difference between proteins and their proteolytic peptides in the two populations can be detected by MS. The ratio of peak intensities in the mass spectrum for the labeled versus unlabeled forms reflect the relative protein abundances in the two samples. This approach delivers the highest precision because the label is incorporated before any analytical steps are undertaken, and it therefore accounts for sample handling biases through the whole analytical process. These advantages are in part offset by the cost of the strategy and the fact that the metabolic labeling approach is far from widely applicable. For example, it cannot be applied to the assessment of protein differences in biological fluids collected from human subjects.

Chemical Labeling

Because metabolic labeling is often not feasible, if a stable-isotope label is to be used, it must be introduced later in the workflow by chemically tagging peptides or proteins. Two basic strategies are commonly adopted, as discussed below.

Isotopic Labeling
The many variants of this general strategy all aim to add isotopic atoms or isotope-coded tags to peptides or proteins. Some are simple in concept whereas others combine multiple elements to react with differentially tagged and selectively recovered peptides. Once again, two separate samples are differentially tagged with isotopic labels, mixed, and analyzed. Labeling strategies include enzymatic labeling with ^{18}O at the C-terminus of proteolytic peptides (29); global internal standard technology (GIST), in which deuterated acylating agents (for example, *N*-acetoxy-succinimide [NAS]) are used to label primary amino groups on digested peptides (30); and chemical labeling with formaldehyde in deuterated water, to label primary amines with deuterated methyl groups (31).

Commercial isotopic labeling reagents are also available. The best known commercial option is, perhaps, the isotope-coded affinity tag (ICAT) method (32). Several iterations of ICAT tags have emerged. The first generation of the reagent comprises three separate parts: a sulfhydryl-reactive chemical crosslinking group, a linker, and a biotin entity. The reagent's two versions are an unlabeled form and a heavy form incorporating eight deuterium atoms. The sulfhydryl-reactive group reacts with free thiols (that is, on cysteine residues); the biotin tag is used to selectively recover

the tagged peptides (that is, through binding with avidin); and the linker provides the opportunity to differentially (mass) label two samples. Since not all proteins contain a cysteine residue, this approach is limited in that about 20% of the proteome may be missed. Furthermore, the incorporation of deuterium as the label is suboptimal because of a discernible isotope effect, which manifests itself as differences in retention time. A variant ICAT reagent incorporating ^{13}C was reported several years later (33). A further refinement of the same basic strategy, isotope-coded protein labeling (ICPL), which tags lysine residues and the N-terminus on the intact proteins has also been reported (34). Importantly, ICPL allows the simultaneous comparison of three groups in a single experiment (that is, $[^2H_7]$, $[^2H_3]$, and $[^2H_0]$ forms).

Isobaric Labeling

These are the most commonly used isotope tags. *Isobaric labels* are a set of matched reagents designed to react with peptides to give products of identical masses and chemical properties. Signifi-

cantly, these products can incorporate carefully selected combinations of heavy and light isotopes. Although many different manifestations of isobaric labels exist, they all comprise the same basic components. Those components are a reactive moiety that functionalizes groups such as primary amines or cysteines, a mass reporter with a unique number of isotopic substitutions, and a mass normalizer with a unique mass that balances or equalizes the mass of the tag. Each different tag is designed to be of equal mass when bound to a peptide, but to cleave on collision-induced dissociation (CID) at a specific linker location, thereby delivering different-sized tags (reporters) that can be quantified independently. In a typical workflow, the proteins in various samples are isolated, enzymatically digested to peptides, and labeled with different isobaric tags. The separately labeled samples are then mixed and analyzed as one. On LC–MS analysis, the peptides are separated, fragmented to produce sequence-specific product ions, to determine sequence, and the abundances of the reporter tags are used to determine

the relative amounts of the peptides in the original samples. Commercially available isobaric mass tags (for example, TMT and iTRAQ) allow the simultaneous analysis of multiple samples in one run (such as 4, 6, or 8 mass-unit differences).

Critical Evaluation

Labeled approaches to global protein quantification offer relatively high precision and multiplexing capability, and they suit many sample types. Nevertheless, they are based on the assumption that analytes will be quantitatively — or at least uniformly — labeled in all samples. Because these strategies are based on measuring proteolytic peptides as surrogates of proteins, the general considerations raised previously (that is, the assumption of complete digestion and selection of diagnostic peptides) apply to all of these methods.

Targeted Protein Quantification

Approaches to targeted protein quantification similarly can be divided into two distinct groups: those that detect and

quantify intact proteins (typically by MALDI) and those that quantify one or more surrogate peptides derived from each protein (typically by LC–MS-MS).

Intact Protein Quantification

Although numerous investigators have demonstrated the ability of MALDI as a precise and accurate approach to protein quantification (35–37), the most powerful and widely adopted manifestation of MALDI protein quantification is the mass spectrometric immunoassay. Developed by Nelson and colleagues (38), this assay combines immunoaffinity column capture with MALDI detection and quantification to reduce the number of components in the sample. In contrast to a conventional ELISA, selectivity is achieved through both the antibody and mass-specific detection. In practice, the sample is passed through an immunoaffinity column; the column is washed, to remove other components; and the bound antigen is eluted directly onto a MALDI target, ready for MS.

For quantification by mass spectrometric immunoassay, fixed amounts of a modified form of the antigen, or a similar protein, are typically added to the sample early in the process, as an internal standard. Absolute quantification is possible by reference to a calibration curve prepared and run in concert with the samples. Mass spectrometric immunoassay offers high-throughput protein quantification. It is important to note that it can also provide details about PTMs and genetic variants. In fact, not only is it possible to identify protein heterogeneity, but the variant forms of the same protein can be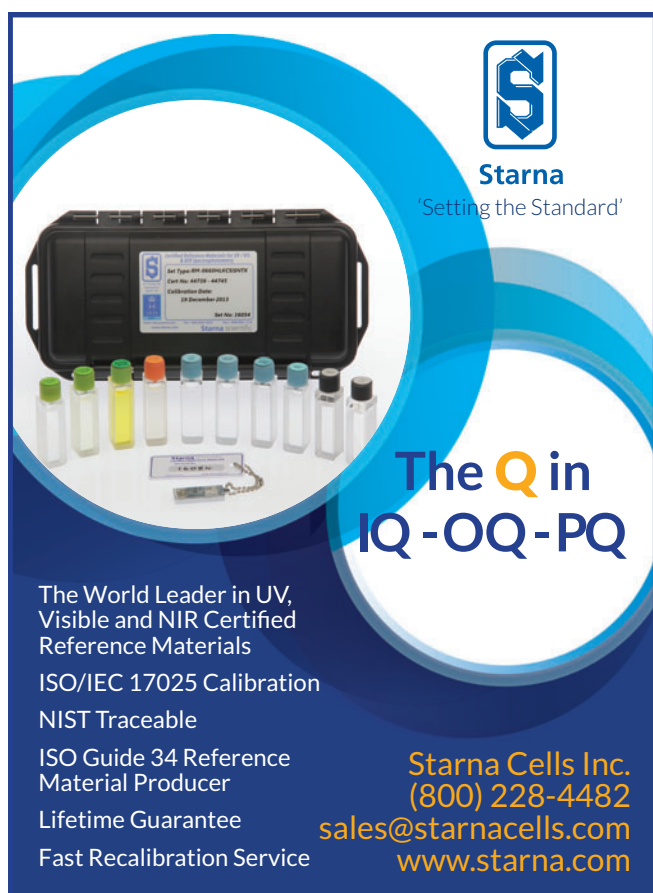 independently quantified. Several different antibodies can be combined in a single column, to allow multiplexed antigen quantification. Although mass spectrometric immunoassay is most commonly combined with MALDI, ESI-based methods have also been developed (39).

Multiple Reaction Monitoring Approaches

Targeted quantification of proteins following their proteolysis to constituent peptides has increasingly become a routine task (40). With a few significant modifications, the process follows the same strategy, essentially, as that described earlier for "label-free methods." First, the target peptides are monitored in MRM mode. Then stable, isotope-labeled versions of the target proteolytic peptides are typically added as an internal standard (though the approach has also been used without incorporating an isotopic internal standard) (41). Monitoring more than one MS-MS transition for each target species provides a powerful approach to quantify a predetermined set of proteins for multiple samples, and it can potentially offer precise and accurate, absolute quantification. Each target protein is cleaved to yield peptides, many of which have a unique sequence (that is, signature, or "proteotypic" peptides). A stable, isotope-labeled version of each signature peptide, designed to be identical to the tryptic peptides generated during digestion, is added at a fixed concentration to each sample, to serve as an internal standard. Because the labeled peptides are coeluted with the target peptide, the internal standards enter the mass spectrometer at the same time as the sample-derived peptides, and therefore they can be concomitantly analyzed by MS-MS. Typically, this approach is performed on a triple-quadrupole mass spectrometer or a hybrid (for example, a quadrupole combined with time-of-flight [TOF] or orbital ion trap analyzer). The target peptide concentration is determined by measuring its observed signal response relative to that of the stable-isotope internal standard. Absolute concentrations can be calculated referring to a calibration curve prepared at the same time. (Calibration curves must be generated for each target peptide in the sample.) With thoughtful selection of the target peptides, it is possible to quantify a specific protein or even a modified form of that protein. No antibody is required, and the process can be performed simultaneously on multiple — even hundreds of — peptides. Therefore, multiple proteins can be quantified in a single LC–MS-MS run. A variant of this process, known as *parallel reaction monitoring* (PRM), allows simultaneous monitoring of all product ions of a target peptide, rather than only a few predetermined transitions (42).

Critical Considerations

Selection of the specific peptides is a central issue because they should be diagnostic of the full target protein; use of just one or two peptides can lead to overestimations of proteins (15). (As discussed previously, target peptides could be common to known variants of the same protein.) Other important considerations address the possibility of incomplete digestion and the fact that sensitivity can be limited in the case of low-abundance proteins without an isolation or enrichment step. A major benefit of this strategy is that cost-effective, precise, and accurate analysis is possible without access to immunoreagents. Yet the approach can prove costly because of the requirement for multiple, stable, isotope-labeled peptides for each target protein. It can also prove time-consuming, because of

the need to analyze the potentially complex MRM data.

Stable-Isotope Standard Capture with Antipeptide Antibodies

Stable-isotope standard capture with antipeptide antibodies (SISCAPA) is essentially the same procedure as that described above, except that it incorporates a specific, antipeptide antibody capture step for the signature peptide and its companion internal standard (43). The additional step enriches the sample for the target peptide and stable isotope standard. At the same time, it provides an opportunity to deplete the sample of interferents, including other peptides generated during the digestion. Importantly, because the internal standard is a perfect mimic of the target peptide, the peptide-to-internal standard ratio is preserved throughout the workup process. Extensive washing can be undertaken, to remove other peptides and clean the sample, without introducing additional variability in the results. The sample is then resolved by a short reversed-phase LC separation and analyzed by LC–MS-MS. Ions characteristic of the target peptide and its corresponding internal standard are monitored in MRM mode. From the signature peptide-to-internal standard ratio, the concentration of the peptide can be calculated by reference to a calibration curve.

Critical Evaluation

Antibody quality is important. So, too, is the selection of the specific peptides. The use of a single peptide is fraught with problems discussed above. The limit of detection is improved because of the opportunity to trap and enrich the target peptides, but the cost and complexity of the approach is increased by the inclusion of this step.

Conclusions

MS quantification is not a trivial undertaking, even for small molecules. When the task at hand is the quantification of hundreds to thousands of proteins in a single sample, the complexity of the analysis is even greater. Shortcuts compromise the process and lead to unsatisfactory and irreproducible results. Nevertheless, with proper care, reflection upon sources of variance, and attention to generating reproducible results, multicomponent protein quantification fit for specific purposes are possible.

References

(1) J.R. Coorssen et al., *Anal. Biochem.* **307**(1), 54–62 (2002).

(2) E. Engvall, K. Jonsson, and P. Perlmann, *Biochim. Biophys. Acta* **251**(3), 427–434 (1971).

(3) E. Engvall and P. Perlmann, *Immunochemistry* **8**(9), 871–874 (1971).

(4) M. Cretich, F. Damin, and M. Chiari, *Analyst* **139**(3), 528–542 (2014).

(5) D.A. Hall, J. Ptacek, and M. Snyder, *Mech. Ageing Dev.* **128**(1), 161–167 (2007).

(6) T. Joos, *Expert Rev. Proteomics* **1**(1), 1–3 (2004).

(7) D. Stoll et al., *Front Biosci.* **7**, c13–32 (2002).

(8) S.C. Tao, C.S. Chen, and H. Zhu, *Comb. Chem. High Throughput Screen* **10**(8), 706–718 (2007).

(9) M.F. Templin et al., *Trends Biotechnol.* **20**(4), 160–166 (2002).

(10) M. Nikolov, C. Schmidt, and H. Urlaub, *Methods Mol. Biol.* **893**, 85–100 (2012).

(11) M. Bantscheff et al., *Anal. Bioanal. Chem.* **404**(4), 939–965 (2012).

(12) K.M. Coombs, *Expert Rev. Proteomics* **8**(5), 659–677 (2011).

(13) W. Zhu, J.W. Smith, and C.M. Huang, *J. Biomed. Biotechnol.* **2010**, 840518 (2010).

(14) M.W. Duncan, R. Aebersold, and R.M. Caprioli, *Nat. Biotechnol.* **28**(7), 659–664 (2010).

(15) M.W. Duncan, A.L. Yergey, and S.D. Patterson, *Proteomics* **9**(5), 1124–1127 (2009).

(16) M. Unlu, M.E. Morgan, and J.S. Minden, *Electrophoresis* **18**(11), 2071–2077 (1997).

(17) A. Alban et al., *Proteomics* **3**(1), 36–44 (2003).

(18) M.W. Duncan and S.W. Hunsucker, *Exp. Biol. Med.* (Maywood) **230**(11), 808–817 (2005).

(19) J.F. Timms and R. Cramer, *Proteomics* **8**(23–24), 4886–4897 (2008).

(20) S.W. Hunsucker and M.W. Duncan, *Proteomics* **6**(5), 1374–1375 (2006).

(21) J.C. Tran et al., *Nature* **480**(7376), 254–258 (2011).

(22) A.I. Nesvizhskii and R. Aebersold, *Mol. Cell. Proteomics* **4**(10), 1419–1440 (2005).

(23) B. Zybailov et al., *J. Proteome Res.* **5**(9), 2339–2347 (2006).

(24) P. Lu et al., *Nat. Biotechnol.* **25**(1), 117–124 (2007).

(25) L. Arike and L. Peil, *Methods Mol. Biol.* **1156**, 213–222 (2014).

(26) M.M. Matzke et al., *Proteomics* **13**(3–4), 493–503 (2013).

(27) D.B. Friedman et al., *Proteomics* **11**(8), 1371–1381 (2011).

(28) S.E. Ong et al., *Mol. Cell Proteomics* **1**(5), 376–386 (2002).

(29) O.A. Mirgorodskaya et al., *Rapid Commun. Mass Spectrom.* **14**(14), 1226–1232 (2000).

(30) A. Chakraborty and F.E. Regnier, *J. Chromatogr. A* **949**(1–2), 173–184 (2002).

(31) J.L. Hsu et al., *Anal. Chem.* **75**(24), 6843–6852 (2003).

(32) S.P. Gygi et al., *Nat. Biotechnol.* **17**(10), 994–999 (1999).

(33) E.C. Yi et al., *Proteomics* **5**(2), 380–387 (2005).

(34) A. Schmidt, J. Kellermann, and F. Lottspeich, *Proteomics* **5**(1), 4–15 (2005).

(35) X. Tang et al., *Anal. Chem.* **68**(21), 3740–3745 (1996).

(36) M. Bucknall, K.Y.C. Fung, and M.W. Duncan, *J. Am. Soc. Mass Spectrom.* **13**(9), 1015–1027 (2002).

(37) A.S. Benk and C. Roesli, *Anal. Bioanal. Chem.* **404**(4), 1039–1056 (2012).

(38) R.W. Nelson et al., *Anal. Chem.* **67**(7), 1153–1158 (1995).

(39) S. Peterman et al., *Proteomics* **14**(12), 1445–1456 (2014).

(40) A.J. Percy et al., *Biochim. Biophys. Acta* **1844**(5), 917–926 (2014).

(41) W. Zhi, M. Wang, and J.X. She, *Rapid Commun. Mass Spectrom.* **25**(11), 1583–1588 (2011).

(42) A.C. Peterson et al., *Mol. Cell. Proteomics* **11**(11), 1475–1488 (2012).

(43) N.L. Anderson et al., *J. Proteome Res.* **3**(2), 235–244 (2004).

(44) M.W. Duncan, A.L. Yergey, and P.J. Gale, *LCGC North Am..* **32**(9), 726–735 (2014).

Mark W. Duncan, PhD, is active in the application of mass spectrometry to the development of biomarkers for disease diagnosis and patient management. He currently works both as an academic in the School of Medicine at the University of Colorado, and as a research scientist at Biodesix Inc., in Boulder, Colorado. He also holds a visiting appointment at King Saud University in Riyadh, Saudi Arabia. **Alfred L. Yergey, PhD,** obtained a B.S in chemistry from Muhlenberg College and his PhD in chemistry from The Pennsylvania State University. He completed a postdoctoral fellowship in the Department of Chemistry at Rice University. He joined the staff of the National Institute of Child Health and Human Development (NICHD), NIH in 1977 from which he retired in 2012 as Head of the Section of Metabolic Analysis and Mass Spectrometry and Director of the Institute's Mass Spectrometry Facility. Yergey was appointed as an NIH Scientist Emeritus upon retirement and maintains an active research program within the NICHD Mass Spectrometry Facility. **P. Jane Gale, PhD,** is currently Director of Educational Services at Waters Corporation. She has spent her career working in the field of mass spectrometry, first at RCA Laboratories and later at Bristol-Myers Squibb, where she was responsible for overseeing the development of quantitative bioanalytical assays to support clinical trials. She is a long-time member of the American Society for Mass Spectrometry (ASMS) and, together with Drs. Duncan and Yergey, created and taught the course in Quantitative Analysis given by the society at its annual conference for nearly a decade. ∎

For more on mass spectrometry, see the full "MS–The Practical Art" column at www.chromatographyonline.com/MSPA. Also, see our ongoing supplement series, Current Trends in Mass Spectrometry, under "Publications," then "Supplements."

PRODUCTS & RESOURCES

FT-IR spectrometer

Agilent's Cary 610 and 620 Fourier transform infrared (FT-IR) systems are designed for applications including biomedical, materials, polymers, food, forensics, pharmaceutical, and chemical applications. According to the company, the systems' IR high-magnification optics provide an additional 5× magnification without changing the objectives.

Agilent Technologies, Santa Clara, CA; www.agilent.com
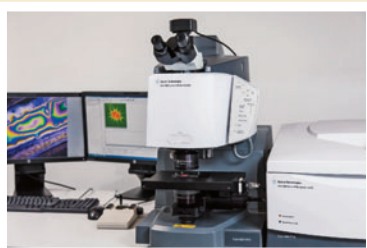
Silicon drift detector

The Fast SDD silicon drift detector from Amptek is designed to provide count rates greater than 1,000,000 counts per second while maintaining resolution. According to the company, the resolution is the same as that supplied by the standard silicon drift detector (125 eV FWHM at the Mn Ka line), and the typical peak-to-background ratio of 20,000:1 is the same, but at a higher count rate.

Amptek Inc., Bedford, MA; www.amptek.com
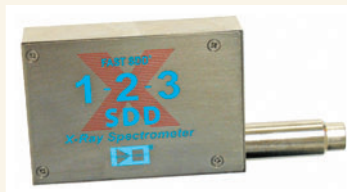
Imaging spectrograph

The Andor Holospec imaging spectrograph is designed for applications such as weak nanostructure photoluminescence, micro-Raman mapping (including TERS), spectrally assisted microfluidics, real-time medical diagnosis, standoff chemical detection, and on-line process control. According to the company, the spectrograph's rugged and compact design make it suitable for challenging industrial or in-the-field applications.

Andor Technology, Belfast, UK; www.andor.com

Fiber probe couplers

FlexiSpec fiber probe couplers from art photonics GmbH are designed to provide efficient coupling of various fiber probes with FT-spectrometers for in-line reaction monitoring in any part of the 0.2–17 µm spectral range. According to the company, the probe couplers enable remote process spectroscopy for liquid, gaseous, and solid media under harsh conditions.

art photonics GmbH, Berlin, Germany; www.artphotonics.com
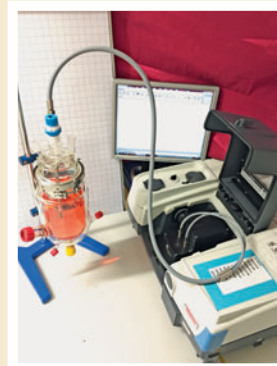
Raman spectrometer

The AvaRaman Supreme Raman spectrometer from Avantes is designed for fast and easy measuring. According to the company, various probes are available for use with the miniature Raman spectroscopy system.

Avantes, Inc., Broomfield, CO; www.avantes.com

Handheld Raman analyzer

The TacticID handheld Raman analyzer from B&W Tek is designed with enhancements in user safety, mixture analysis, and library volume. According to the company, the analyzer offers remote operation and scan delay safety features, advanced chemometric mixture analysis capabilities, and a library of nearly 1000 narcotics, pharmaceutical drugs, cutting agents, and precursors.

B&W Tek, Newark, DE; www.bwtek.com

Mid-IR sources

Compact industrial-grad mid-IR sources from Cobolt are reportedly based on a fully contained temperature-tunable optical parametric oscillator with an integrated pump laser. According to the company, the sources are wavelength-selectable from 2 µm to 5 µm, tunable up to 40 nm, and provide up to 80 mW at 10 kHz.

Cobolt, Solna, Sweden; www.cobolt.se

Spectrofluorometer

The FS5 spectrofluorometer from Edinburgh Instruments is designed for research and analytical applications. According to the company, the spectroflurometer has fluorescence and phosphorescence measurements capability, including lifetimes, up to 1650 nm, and a transmission detector for UV–vis absorption spectroscopy is included.

Edinburgh Instruments, West Lothian, UK; www.edinst.com

ICP spray chamber

The IsoMist programmable-temperature spray chamber accessory from Glass Expansion is designed to be used for either heating or cooling the spray chamber with a range of -10 to +60 °C. According to the company, heating the spray chamber provides control of viscosity and sample transport to optimize the delivery of difficult samples.
Glass Expansion, Pocasset, MA; www.geicp.com

CCD camera

The Syncerity back-illuminated, deep-cooled CCD camera from Horiba is designed for OEM and research vis–NIR spectroscopy applications. According to the company, the camera has an NIR-enhanced 2048 × 70 sensor, and its high-resolution 14-µm pixel size makes it suitable for use in Raman instrumentation.
Horiba Scientific, Edison, NJ; www.horiba.com

UV–vis spectrophotometers

JASCO's V-700 UV–vis and NIR spectrophotometers are designed for high-speed scanning and feature a range of application-specific accessories and software. Two graphical user interfaces reportedly are available, including the latest version of the company's Spectra Manager II cross-platform spectroscopy software for full system control and advanced data processing.
JASCO, Easton, MD; www.jascoinc.com/uv-vis

Helium neon lasers

Helium neon lasers from Melles Griot are designed in a range of HeNe wavelengths with random or linear polarized output. According to the company, the lasers are available at 632.8, 543.5, and 594.1 nm with up to 35 mW of output power (wavelength dependent) including self-contained and frequency stabilized systems in compact packages, plasma tubes, or fully customized configurations for OEMs.
Melles Griot, Carlsbad, CA; www.mellesgriot.com

Raman spectroscopy brochure

A brochure from Ocean Optics provides information about the company's Raman products and their applications. The brochure reportedly contains a comparison of modular Raman spectrometers and turnkey Raman systems; application and technical notes; customized solutions for OEM; and information about IDRaman products and raster orbital scanning, SERS substrates, and more.
**Ocean Optics,** Dunedin, FL; www.oceanoptics.com

Data analysis and graphing software

Origin and OriginPro 2015, the latest version of OriginLab's data analysis and graphing software, is designed with more than 100 new features and improvements added to version 9.1. According to the company, key enhancements include collapsible menus, project file search for string, thumbnail previews of graphs, and tooltips displaying folder or window comments in Project Explorer, and choice of icon-or details-listing of project contents.
OriginLab, Northampton, MA; www.originlab.com
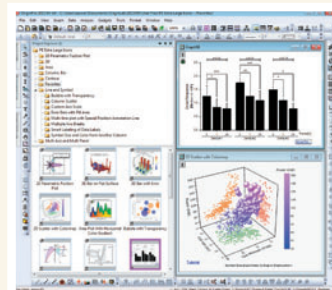
Ion beam profiler

A digital ion beam-profiling unit from Photonis reportedly combines a large microchannel plate (up to 120 mm) in a complete assembly with the company's high-resolution digital CMOS low-light camera. According to the company, the camera is immune to sudden light damage and a diagnostic tool allows the instrument to be designed to maximize the amount of ions collected.
**Photonis USA,** Sturbridge, MA; www.photonis.com

Raman imaging option

Renishaw's Stream-LineHR Rapide option for its inVia Raman microscope is designed to enable the rapid collection of large amounts of Raman data. According to the company, with this capability, users can generate high definition chemical images quickly with a detector spectrum readout rate of over 1000 s^{-1}.
**Renishaw,** Hoffman Estates, IL; www.renishaw.com/raman
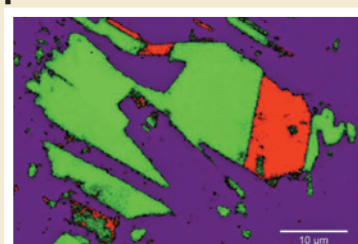
Hyperspectral imager

BaySpec's OCI-U hyperspectral camera is designed for high-speed, compact, portable, or in-line imaging systems. According to the company, the camera's miniature single-board computer acquires vis-NIR hyperspectral data with continuous spectral and spatial coverage.
BaySpec, Inc.,
San Jose, CA;
www.bayspec.com
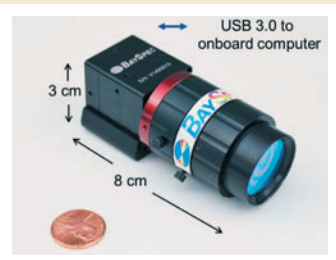
Grinder

Retsch's RS 200 vibratory disk mill grinder is designed with an ergonomic carry handle to facilitate carriage of the heavy grinding jar. According to the company, a clamping device allows for safe clamping of the jar with less force, and an additional sensor checks its correct position.
Retsch,
Newtown, PA;
www.retsch-us.com

Atomic emission spectrometers

Shimadzu's ICPE-9800 series Simultaneous ICP atomic emission spectrometers are designed for chemical, environmental, pharmaceutical, food, metal, and electronics analysis. According to the company, the spectrometers feature a charge-coupled device detector with one million pixels.
Shimadzu Scientific Instruments,
Columbia, MD;
www.ssi.shimadzu.com

ICP-OES whitepaper

A whitepaper authored by Spectro Analytical Instruments reportedly details how new ICP-OES spectrometer technologies are cutting operating costs in environmental, industrial, and academic laboratories. According to the company, the whitepaper is available to download at http://icp-oes.spectro.com/blue.
Spectro Analytical Instruments,
Mahwah, NJ;
www.spectro.com
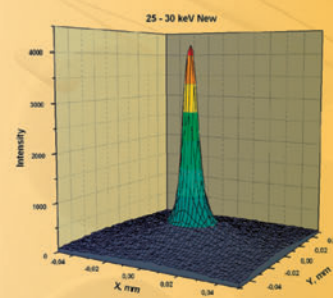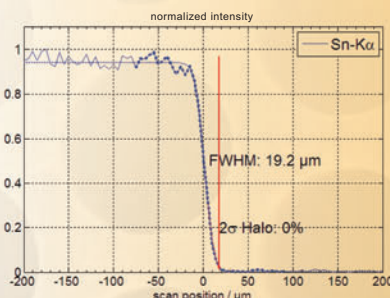
Raman spectrometers

Updated Raman spectrometers from StellarNet are configured for quick identification of a variety of liquid, solid, and powder samples. According to the company, all Raman spectrometers can be coupled to its StellarScope microscope system.
StellarNet, Inc., Tampa FL; www.StellarNet.us

Mercury analyzers

Mercury analyzers available from Teledyne Leeman Labs include the company's Hydra II mercury analyzers as well as the QuickTrace mercury analyzers previously produced by Teledyne CETAC Technologies. According to the company, the consolidated product line will consist of the QuickTrace M-8000 cold vapor atomic fluorescence system and the Hydra II and QuickTrace M-7600 cold vapor atomic absorption systems, all for liquid samples. The Hydra II C analyzer for semisolid samples will also be available.
Teledyne Leeman Labs, Hudson, NH; www.teledyneleemanlabs.com

3D Raman imaging

WITec's alpha300 Raman microscope is designed for diffraction-limited and ultrafast 3D Raman imaging to be performed routinely and simultaneously. According to the company, combination possibilities with SEM, AFM, and profilometry for correlative microscopy in an integrated system provide a comprehensive sample characterization from the millimeter to the nanometer range.
WITec GmbH, Ulm, Germany; www.witec.de

Data analysis database

International Centre for Diffraction Data's PDF-4+ 2014 database is designed for both phase identification and quantitative analysis. According to the company, the database provides material coverage for inorganic materials with 354,264 entries and supports automated quantitative analyses by providing key reference data required for these analyses.
ICDD, Newtown Square, PA; www.icdd.com

Fiber-coupled LEDs

The FCS fiber-coupled LEDs from Moxtek are designed to achieve a high optical output power. According to the company, the output has an SMA connection that allows the unit to be compatible with any SMA fiber, and several wavelengths are available within a range of 240–940 nm. The LEDs feature an electrical locking mechanism and mounting holes that reportedly make it suitable for laboratory, industrial, and OEM applications.
Mightex, Pleasanton, CA; www.mightex.com

FT–IR spectrometer

Bruker's Tensor II FT-IR spectrometer is a compact, research-grade instrument designed for use in advanced FT-IR applications in research and development, routine quality control applications, and material verification. According to the company, the spectrometer uses a diode laser with a hold time that is longer than that of HeNe lasers included in conventional R&D FT-IR instrumentation.
**Bruker Corporation,** Billerica, MA; www.bruker.com

Raman filters

A set of BragGrate Raman filters from Optigrate are designed to enable access to Stokes and anti-Stokes Raman bands in the ultralow frequency terahertz region (5–200 cm^{-1}). According to the company, filter set includes a laser line cleaning filter and light rejection notch filters with the linewidth narrower than 5 cm^{-1}.
Optigrate, Oviedo, FL; www.optigrate.com
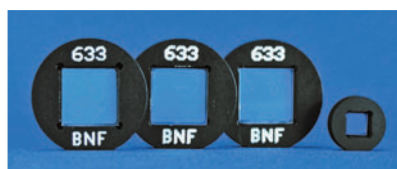
Mid-IR integrating spheres

Integrating spheres from PIKE Technologies are designed for use with FT-IR spectrometers. According to the company, the spheres feature a 3-in. diameter reflective gold-coated surface and are available in upward- and downward-looking configurations.
PIKE Technologies, Madison, WI; www.piketech.com

Miniature X-ray source

Moxtex's 12 W miniature X-ray source is designed with a higher voltage and higher emission current than the company's present miniature X-ray sources. According to the company, the source operates at high voltages up to 60 kV, low voltages of 4 kV, and emission currents up to 1.0 mA.

Moxtek, Inc.,
Orem, UT;
www.moxtek.com

WDXRF spectrometer

The Supermini200 wavelength dispersive X-ray fluorescence spectrometer from Rigaku is designed for elemental analysis. According to the company, no chemical preparation step is required, and the spectrometer has light element sensitivity and low limits of detection.

Rigaku Corporation,
Tokyo, Japan;
www.rigaku.com

PFA cyclonic spray chamber

The PFA cyclonic spray chamber from Savillex is designed to provide stability and sensitivity for ICP-OES and ICP-MS applications. According to the company, translucent walls allow the user to see inside the chamber during operation, and a smooth surface finish helps improve washout.

Savillex Corporation,
Eden Prairie, MN;
www.savillex.com

Diamond antireflection coating

The Diamond XP-BBAR coating from Spectral Systems is designed to provide throughput and performance increase in the infrared spectral region. According to the company, the coating can be applied to both surfaces of a diamond window or input and exit surfaces of a diamond ATR optical element.

Spectral Systems, Inc.,
Hopewell Junction, NY;
www.spectral-systems.com

Benchtop Raman micro-spectroscopy system

The uRaman Raman spectroscopy system from TechnoSpex is designed to integrate Raman technology into an existing upright microscope. According to the company, the modular unit is compatible with existing upright microscope functions such as phase contrast, dark field, DIC, and polarization imaging, and users can purchase one excitation laser and then add on another laser wavelength by stacking modules.

TechnoSpex Pte Ltd., Singapore;
www.technospex.com
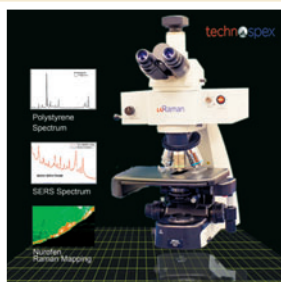
Handheld LIBS analyzer

The Z handheld LIBS spectrometer from SciAps is designed to provide comparable performance to silicon drift detector–based HHXRF analyzers. The spectrometer reportedly can measure carbon and many other low-atomic number elements. According to the company, the analyzer uses an eye-safe laser technology that allows the use of high-energy laser pulses (>4 mJ) while retaining a Class 1 laser rating.

SciAps,
Woburn, MA;
www.sciaps.com

Mass spectrometer

Thermo Fisher Scientific's Q Exactive Focus LC–MS-MS system is designed for laboratories performing food and environmental testing clinical research, forensic toxicology, pharmaceutical and biopharmaceutical measurements, and other applied analyses. According to the company, the orbital ion trap–based instrument delivers up to 70,000 resolution at *m/z* 200, and a scan speed of up to 12 Hz.

Thermo Fisher Scientific,
San Jose, CA;
www.thermofisher.com/qefocus

Laboratory-based LIBS analyzers

ChemReveal laboratory-based analyzers from TSI are designed to use laser-induced breakdown spectroscopy to provide identification of materials and chemical composition of solids. According to the company, the analyzers are equipped with the company's ChemLytics software.

TSI Incorporated,
St. Paul, MN;
www.tsi.com/ChemReveal

Calendar of Events

January 2015

22–25 Security and Forensic Applications of Mass Spectrometry
Clearwater Beach, FL
www.asms.org/conferences/sanibel-conference/sanibel-conference-homepage

25–28 29th International Forum on Process Analytical Chemistry (IFPAC 2015)
Arlington, VA
www.ifpac.com

29 January – 1 February 62nd Pacific Conference on Spectroscopy and Dynamics
Pacific Grove, CA
www.westernspectroscopy.org

February 2015

7–11 Society for Laboratory Automation and Screening 4th Annual Conference and Exhibition (SLAS2015)
Washington DC
www.slas2015.org

7–11 Biophysical Society 59th Annual Meeting
Baltimore, MD
www.biophysics.org/2015meeting/Exhibits/InterestedinExhibiting/tabid/4900/Default.aspx

7–12 SPIE Photonics West
San Francisco, CA
spie.org/x2584.xml

9–12 PANIC 2015 – Practical Applications of NMR in Industry Conference
La Jolla, CA
www.panicnmr.com

22–26 European Winter Conference on Plasma Spectrochemistry
Münster, Germany
www.ewcps2015.org

26 February–3 March 14th International Conference on Particle Induced X-Ray Emission (PIXE 2015)
Somerset West, South Africa
www.pixe2015.tlabs.ac.za

March 2015

1–4 FTS/HISE
Lake Arrowhead, CA
www.osa.org/en-us/meetings/optics_and_photonics_congresses/fts_hise/

2–6 American Physical Society March Meeting
San Antonio, TX
www.aps.org/meetings/march/

8–11 CANAS 2015 – Colloquium Analytical Atomic Spectroscopy
Leipzig, Germany
www.canas2015.org

8–12 The Pittsburgh Conference on Analytical Chemistry and Applied Spectroscopy (PITTCON 2015)
New Orleans, LA
www.pittcon.org

12–14 3rd International Conference on Photonics, Optics and Laser Technology (Photoptics 2015)
Berlin, Germany
www.photoptics.org

22–26 249th American Chemical Society National Spring Meeting & Exposition
Denver, CO
www.acs.org/content/acs/en/meetings/spring-2015.html

23–26 ARABLAB 2015
Dubai, United Arab Emirates
www.arablab.com

29 March–2 April The 48th Annual International Meeting of the ESR Spectroscopy Group of the Royal Society of Chemistry
Winchester, Hampshire, UK
store.southampton.ac.uk/browse/extra_info.asp?compid=1&modid=2&catid=34&prodid=239

31 RSC NMR Discussion Group (NRMDG) Spring Meeting: Diffusion NMR
Birmingham, UK
www.nmrdg.org.uk

April 2015

6–10 Materials Research Society Spring Meeting
San Francisco, CA
www.mrs.org/spring2015

11–14 American Physical Society April Meeting
Baltimore, MD
www.aps.org/meetings/april/

12–15 OSA Topical Meeting: Optics in the Life Sciences
Vancouver, Canada
www.osa.org/en-us/meetings/optics_and_photonics_congresses/optics_in_the_life_sciences/

12–15 European Conference on Nonlinear Optical Spectroscopy (ECONOS 2015)
Leuven, Belgium
www.econos2015.org

Short Courses

February 2015

24–26 7th European Short Course on Time-Resolved Microscopy and Correlation Spectroscopy
Berlin, Germany
www.picoquant.com/events/details/microscopy-course

March 2015

7–8 Application of Inductively Coupled Plasma Atomic Emission (ICP-AES) Spectrometry
New Orleans, LA
ca.pittcon.org/Technical+Program/tpab-stra15.nsf/SCoursesByCat/B0C5006AB0FBD6B485257CFF004AA700?opendocument

7 Accessories and Techniques for FT-IR Sample Analysis
New Orleans, LA
ca.pittcon.org/Technical+Program/tpab-stra15.nsf/SCoursesByCat/86478DA73C82053F85257D08005F0CB4?opendocument

8 Introduction to ICP Mass Spectrometry
New Orleans, LA
ca.pittcon.org/Technical+Program/tpab-stra15.nsf/SCoursesByCat/3F714EE86E2F0ADF85257CF20073F712?opendocument

8 Gas Chromatography/Infrared Spectrometry
New Orleans, LA
ca.pittcon.org/Technical+Program/tpab-stra15.nsf/SCoursesByCat/CF31A92C94CF46A585257CD7005E2D1E?opendocument

9 Handheld Vibrational Spectrometers: State-of-the Art Instrumentation and Novel Applications
New Orleans, LA
ca.pittcon.org/Technical+Program/tpab-stra15.nsf/SCoursesByCat/0E8F1BE6D681B65B85257CE30068E2A6?opendocument

9 Multivariate Calibration as an Aid to Develop Atomic Spectroscopy Methods
New Orleans, LA
ca.pittcon.org/Technical+Program/tpab-stra15.nsf/SCoursesByCat/ADA3B5F0643C723985257CEF005D60AC?opendocument

9 Practical Introduction to Near-Infrared Method Development
New Orleans, LA
ca.pittcon.org/Technical+Program/tpab-stra15.nsf/SCoursesByCat/9BEBEF8560C8483D85257D0F00759C79?opendocument

9 Fundamentals of Particle Size Analysis with an Emphasis on Light Scattering Techniques
New Orleans, LA
ca.pittcon.org/Technical+Program/tpab-stra15.nsf/SCoursesByCat/1FA79345F3EFE6F885257CFB00697045?opendocument

10–11 Atomic Force Microscopy, a Toolkit for Nanoscale Characterization: From Basic Modes to Advanced Applications
New Orleans, LA
ca.pittcon.org/Technical+Program/tpab-stra15.nsf/SCoursesByCat/0196C5E68D3F57AC85257CFC0001FF4F?opendocument

10 LIMS & ELN: How to Select, Plan, and Implement the Right Software for Your Laboratory
New Orleans, LA
ca.pittcon.org/Technical+Program/tpab-stra15.nsf/SCoursesByCat/129CA01E739E624985257CFC00638463?opendocument

10 How to Select an ICP-Mass Spectrometer: The Most Important Analytical Considerations
New Orleans, LA
ca.pittcon.org/Technical+Program/tpabstra15.nsf/SCoursesByCat/15393F680829A5EB85257CF20071C32E?opendocument

10 Particle Size and Zeta Potential Characterization of Nano Particles
New Orleans, LA
ca.pittcon.org/Technical+Program/tpab-stra15.nsf/SCoursesByCat/CBA6FD7E33FA59E285257CFB006E30EB?opendocument

11 Practical Introduction to Near IR and Raman Spectroscopy
New Orleans, LA
ca.pittcon.org/Technical+Program/tpab-stra15.nsf/SCoursesByCat/1918C2E6E929912A85257D01004EBF24?opendocument

11–12 Basic Theory, Instrumentation and Applications of Vibrational Spectroscopy (Raman, Mid-Infrared and Near-Infrared) in Materials Science
New Orleans, LA
ca.pittcon.org/Technical+Program/tpab-stra15.nsf/SCoursesByCat/2A61CA0027EA8B5985257CE30064F48D?opendocument

11 Spectroscopic Measurements of Organic and Inorganic Nanomaterials for Energy
New Orleans, LA
ca.pittcon.org/Technical+Program/tpab-stra15.nsf/SCoursesByCat/8F391BDCB5531EB785257D060082DAC8?opendocument

12 Side Illuminated Optical Fibers as a Multiplexing Element of Spectroscopic Systems
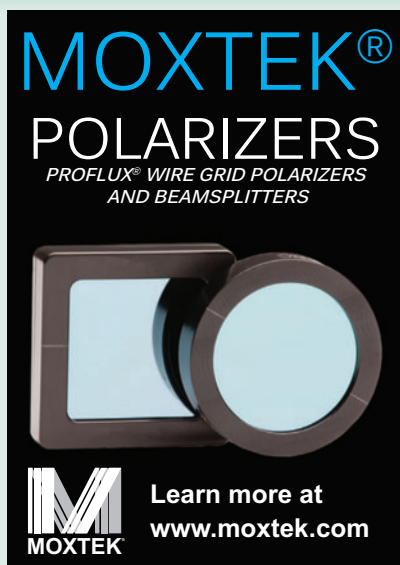New Orleans, LA
ca.pittcon.org/Technical+Program/tpab-stra15.nsf/SCoursesByCat/7C8FC8D08FD7F1A985257D040080429E?opendocument

May 2015

18–22 2015 NIST Spectrophotometry Short Course
Gaithersburg, MD
www.nist.gov/pml/div685/sc/spectrophotometry_course.cfm

Ad Index

Ultra-Low Frequency Raman Spectroscopy

"Extend your Raman system into THz frequency range (5-200 cm^{-1})"

SiGe Superlattice @532 nm

Measured with
LabRAM HR Evolution
*(data courtesy of :
HORIBA Jobin Yvon SAS)*
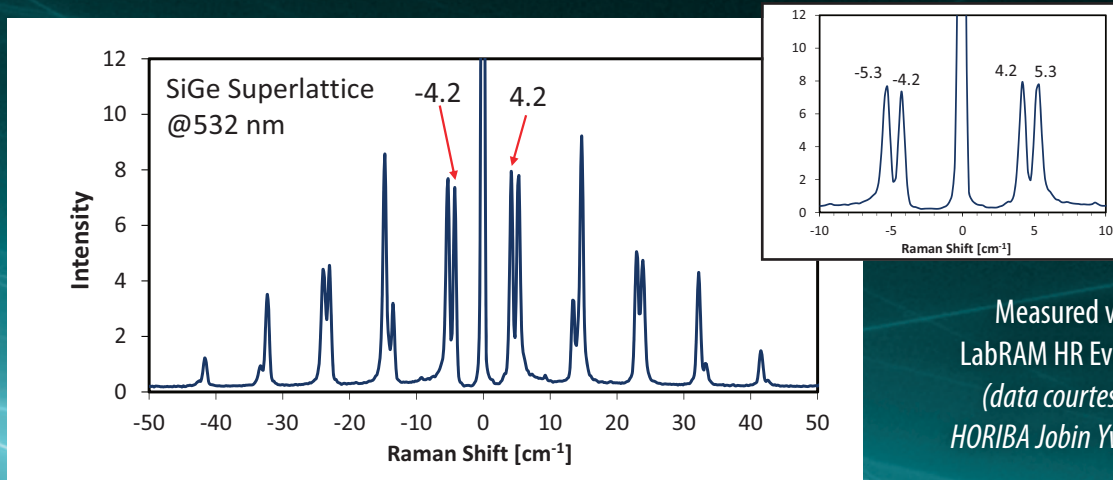
BragGrate™ Bandpass and Notch Filters

Spectral and spatial laser line cleaning filters and ultra-narrow line notch filters for low frequency Raman Spectroscopy

**Wavelengths
in Production (nm)**
405, 442, 458, 473, 488,
491, 514, 532, 552, 561,
568, 588, 594, 632, 660,
785, 830, 980, 1064, 1550

- **Frequencies below 10 cm^{-1} with single stage spectrometer**
- **Angle tunable for precise wavelength adjustment**
- **Stokes and anti-Stokes Raman bands**
- **Unlimited optical life-time**
- **Custom wavelengths in range 400–2000 nm**